

ARMY ENGINEER WATERWAYS EXPERIMENT STATION VICKSBURG--ETC F/G 13/10
NUMERICAL ANALYSIS OF HARBOR RESONANCE RESPONSE IN EAST CHANNEL--ETC(U)
JUN 81 D 6 OUTLAW, J R HOUSTON
WES/MP/HL-81-3 NL

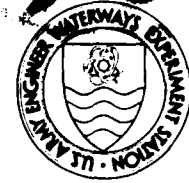
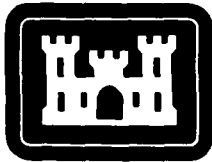
NL

1 of 1
21
Apr 4 2016

END
DATE
FILMED
10-8
DTIC

LEVEL II
150

72



MISCELLANEOUS PAPER HL-81-3

NUMERICAL ANALYSIS OF HARBOR RESONANCE RESPONSE IN EAST CHANNEL LOS ANGELES HARBOR

by

Douglas G. Outlaw, James R. Houston

Hydraulics Laboratory
U. S. Army Engineer Waterways Experiment Station
P. O. Box 631, Vicksburg, Miss. 39180

June 1981

Final Report

Approved For Public Release; Distribution Unlimited

AD A103426



DTIC FILE COPY

Prepared for Port of Los Angeles
San Pedro, Calif. 90733

DTIC
ELECTRIC
S
AUG 28 1981

80 8 28 017

Destroy this report when no longer needed. Do not return
it to the originator.

The findings in this report are not to be construed as an official
Department of the Army position unless so designated.
by other authorized documents.

The contents of this report are not to be used for
advertising, publication, or promotional purposes.
Citation of trade names does not constitute an
official endorsement or approval of the use of
such commercial products.

Unclassified

SECURITY CLASSIFICATION OF THIS PAGE (When Data Entered)

14 WES/MI/HL-131

REPORT DOCUMENTATION PAGE		READ INSTRUCTIONS BEFORE COMPLETING FORM
1. REPORT NUMBER Miscellaneous Paper HL-81-3	2. GOVT ACCESSION NO. AD-4103426	3. RECIPIENT'S CATALOG NUMBER
4. TITLE (and Subtitle) NUMERICAL ANALYSIS OF HARBOR RESONANCE RESPONSE IN EAST CHANNEL, LOS ANGELES HARBOR		5. TYPE OF REPORT & PERIOD COVERED Final report, Jul-Dec. 1981
7. AUTHOR(s) Douglas G. Outlaw James R. Houston		6. PERFORMING ORG. REPORT NUMBER
9. PERFORMING ORGANIZATION NAME AND ADDRESS U. S. Army Engineer Waterways Experiment Station Hydraulics Laboratory P. O. Box 631, Vicksburg, Miss. 39180		8. CONTRACT OR GRANT NUMBER(s)
11. CONTROLLING OFFICE NAME AND ADDRESS Port of Los Angeles P. O. Box 151 San Pedro, California 90733		10. PROGRAM ELEMENT, PROJECT, TASK AREA & WORK UNIT NUMBERS
14. MONITORING AGENCY NAME & ADDRESS (if different from Controlling Office)		12. REPORT DATE June-1981
		13. NUMBER OF PAGES 45
		15. SECURITY CLASS. (of this report) Unclassified
		15a. DECLASSIFICATION/DOWNGRADING SCHEDULE
16. DISTRIBUTION STATEMENT (of this Report) Approved for public release; distribution unlimited.		
17. DISTRIBUTION STATEMENT (of the abstract entered in Block 20, if different from Report)		
18. SUPPLEMENTARY NOTES Available from National Technical Information Service, 5285 Port Royal Road, Springfield, Va. 22151.		
19. KEY WORDS (Continue on reverse side if necessary and identify by block number) Finite element method Harbor oscillations Los Angeles Harbor Mathematical models Numerical analysis		
20. ABSTRACT (Continue on reverse side if necessary and identify by block number) A hybrid finite-element numerical model was used to calculate harbor resonance, relative to that for existing conditions, for proposed non-Federal dredging adjacent to East Channel in the Port of Los Angeles. The numerical model yields convergent solutions for harbors of arbitrary shape and variable depth. The response of East Channel to long-period wave excitation was calculated over the 60- to 600-sec range for each plan. Wave-height amplification-		

(Continued)

Unclassified

SECURITY CLASSIFICATION OF THIS PAGE (When Data Entered)

Unclassified

SECURITY CLASSIFICATION OF THIS PAGE(When Data Entered)

20. ABSTRACT (Continued).

was similar at periods less than 200 sec; however, amplification of the fundamental mode of oscillation (near a period of 6 min for each plan) was significantly different.

Unclassified

SECURITY CLASSIFICATION OF THIS PAGE(When Data Entered)

PREFACE

The investigation reported herein was authorized by the Los Angeles Port Authority under a contract, Agreement No. WES 78-16, dated 15 November 1978.

The investigation was conducted from July 1979 to December 1979 by personnel of the Hydraulics Laboratory, U. S. Army Engineer Waterways Experiment Station (WES), under the direction of Mr. H. B. Simmons, Chief of the Hydraulics Laboratory, Mr. F. A. Herrmann, Jr., Assistant Chief of the Hydraulics Laboratory, Dr. R. W. Whalin, Chief of the Wave Dynamics Division, and Mr. C. E. Chatham, Chief of the Wave Processes Branch. Mr. D. G. Outlaw and Dr. J. R. Houston conducted the investigation and prepared this report. Mrs. M. L. Hampton and Mr. J. Kuhnert aided in development of the finite-element grids and data presentation. Drs. H. S. Chen and C. C. Mei of the Massachusetts Institute of Technology provided documentation of the hybrid finite-element computer program they developed and materials to aid in its utilization.

Commanders and Directors of WES during the investigation and the preparation and publication of this report were COL John L. Cannon, CE, and COL Nelson P. Conover, CE. Technical Director was Mr. F. R. Brown.

Accession For	
NTIS GRA&I	<input checked="checked" type="checkbox"/>
DTIC TAB	<input type="checkbox"/>
Unannounced	<input type="checkbox"/>
Justification	
By	
Distribution/	
Availability Codes	
Dist	Avail and/or Special
A	

DTIC
ELECTE
AUG 28 1981
S D

CONTENTS

	<u>Page</u>
PREFACE	1
PART I: INTRODUCTION	3
Objective	3
Improvement Plans	4
PART II: NUMERICAL MODEL	7
PART III: RESULTS	11
PART IV: CONCLUSIONS	16
PLATES 1-29	
APPENDIX A: NOTATION	A1

NUMERICAL ANALYSIS OF HARBOR RESONANCE
RESPONSE IN EAST CHANNEL, LOS ANGELES HARBOR

PART I: INTRODUCTION

Objective

1. The objective of this study was to investigate the comparative response of East Channel of the Port of Los Angeles (Figure 1) to long-period wave excitation for the existing configuration and for three proposed dredging alternatives near East Channel. Amplification factors were computed as a function of period at the north end of East Channel and the normalized maximum current velocity was computed at the entrance to East Channel and at the Bulk Loading Terminal, berth 50. These data

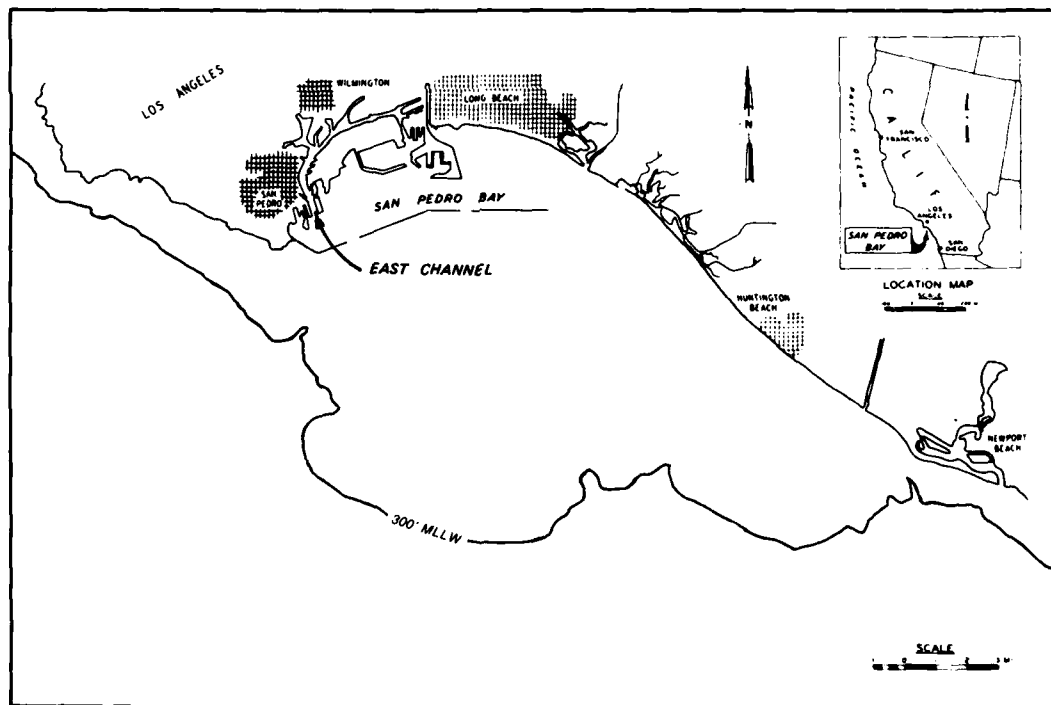


Figure 1. Site map

were plotted to ascertain whether or not significant differences in channel resonance might occur that would potentially impact (either positively or negatively) ship mooring conditions.

2. A previous harbor oscillation study of the Port of Los Angeles* used the same numerical model; however, the previous study considered effects of a more extensive harbor improvement plan and did not include the non-Federal dredging (NFD) investigated herein.

Improvement Plans

3. The following three proposed dredging plans were considered:

<u>Designation</u>	<u>Description</u>
Phase I-B	Federal Project for harbor deepening and associated non-Federal dredging retaining the submerged bar south of pier 1
Phase I-B (NFD-1)	Phase I-B plan with the submerged bar south of pier 1 dredged to -45 ft mllw
Phase I-B (NFD-2)	Phase I-B plan with approximately 70 percent of the seaward end of the submerged bar south of pier 1 dredged to -35 ft mllw

Figures 2-5 illustrate the base plan and the three dredging alternatives.

4. Waves from a southerly direction with periods from 60 to 600 sec were considered. Wave amplitudes and current velocities were calculated at 1- to 10-sec intervals, dependent on the period range. Resonant peaks were defined by using incident wave periods in 0.25-sec increments.

* J. R. Houston. 1977 (Feb). "Los Angeles Harbor Numerical Analysis of Harbor Oscillations," Miscellaneous Paper H-77-2, U. S. Army Engineer Waterways Experiment Station, CE, Vicksburg, Miss.

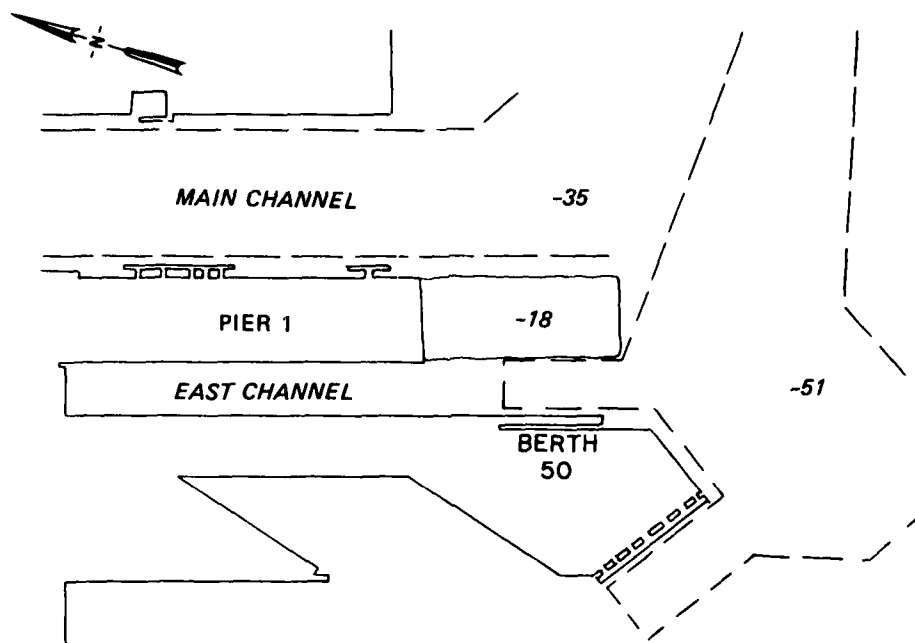


Figure 2. Base plan

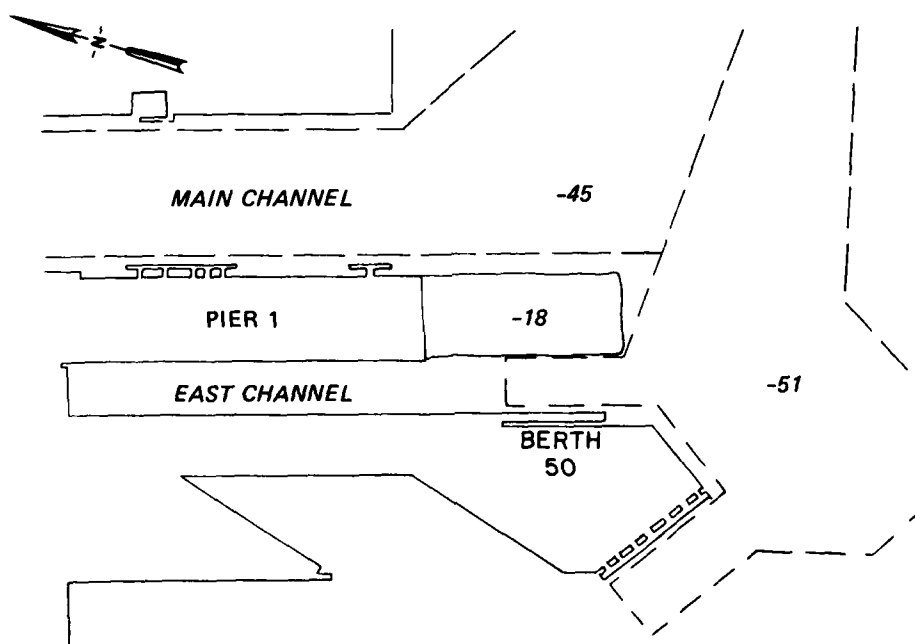


Figure 3. Phase I-B plan

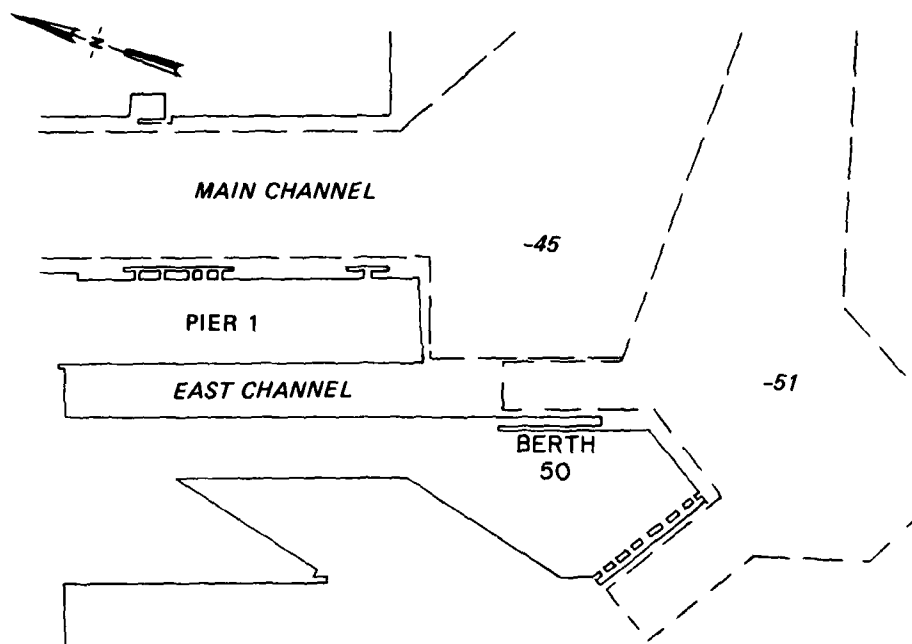


Figure 4. Phase I-B (NFD-1) plan

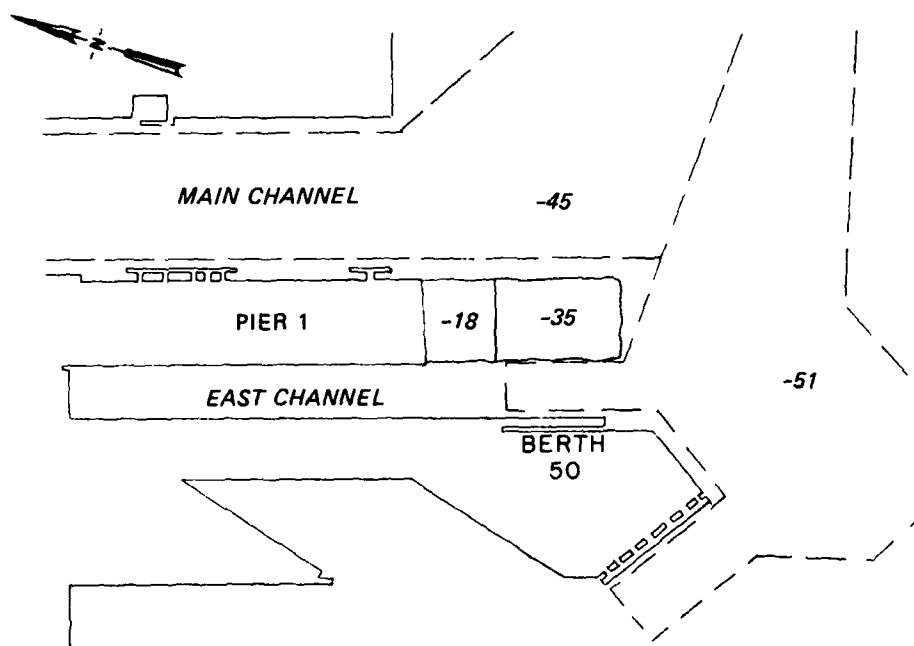


Figure 5. Phase I-B (NFD-2) plan

PART II: NUMERICAL MODEL

5. The response of East Channel to long-wave excitation was determined by using a hybrid finite-element numerical model developed at the Massachusetts Institute of Technology.* The model solves the following generalized Helmholtz equation:

$$\nabla \cdot [h(x,y)\nabla\phi(x,y)] + \frac{\omega^2}{g} \phi(x,y) = 0$$

where ∇ is the gradient operator, $h(x,y)$ is the water depth, $\phi(x,y)$ ** is the velocity potential defined by $U(x,y) = -\nabla\phi(x,y)$, with $U(x,y)$ being a two-dimensional velocity vector, ω is an angular frequency, and g is the acceleration due to gravity. Equation 1 governs small amplitude undamped oscillations of long waves. It has been further assumed that the flow is irrotational.

6. The boundary condition along the shoreline and in the harbor is that the normal component of the velocity be equal to zero.

7. The Helmholtz equation:

$$\nabla^2\phi(x,y) + \frac{\omega^2}{gh} \phi(x,y) = 0 \quad (2)$$

is the governing equation for a constant-depth ocean region outside the basin.

8. For a harbor in a semi-infinite ocean with a straight coastline there are incident, reflected, and scattered waves. The scattered wave has a velocity potential ϕ_s given by

* H. S. Chen and C. C. Mei. 1974 (Aug). "Oscillations and Wave Forces in an Offshore Harbor (Applications of the Hybrid Finite Element Method to Water-Wave Scattering)," Report No. 190, Massachusetts Institute of Technology, Cambridge, Mass.

** For convenience, symbols and unusual abbreviations are listed and defined in the Notation (Appendix A).

$$\phi_s = \sum_{n=0}^{\infty} \alpha_n H_n(kr) \cos n\theta \quad (3)$$

where α_n are unknown coefficients and $H_n(kr)$ are Hankel functions of the first kind of order n .

9. ϕ_s satisfies the radiation condition that the scattered wave must behave as an outgoing wave at infinity. This condition is known as the Sommerfeld radiation condition and may be expressed mathematically as follows:

$$\lim_{r \rightarrow \infty} \sqrt{r} \left(\frac{\partial}{\partial r} - ik \right) \phi_s = 0 \quad (4)$$

10. Chen and Mei used a calculus of variations approach and obtained a Euler-Lagrange formulation of the boundary value problem. The following functional F with the property that it is stationary with respect to arbitrary first variations of $\phi(x,y)$ was constructed by Chen and Mei:

$$\begin{aligned} F(\phi) = & \iint 1/2 \left[h(\nabla\phi)^2 - \frac{\omega^2}{g} \phi^2 \right] dA \\ & + 1/2 \oint \left[h(\phi_R - \phi_I) \frac{\partial(\phi_R - \phi_I)}{\partial n_a} \right] da - \oint \left[h\phi_a \frac{\partial(\phi_R - \phi_I)}{\partial n_a} \right] da \\ & - \oint \left(h\phi_a \frac{\partial\phi_I}{\partial n_a} \right) da + \oint \left[h\phi_I \frac{\partial(\phi_R - \phi_I)}{\partial n_a} \right] da \end{aligned} \quad (5)$$

where

A = region inside the harbor

\oint = line integral

ϕ_R = far field velocity potential

ϕ_I = velocity potential of the incident wave

n_a = unit normal vector outward from region A

a = boundary of region A

ϕ_a = total velocity potential evaluated on boundary a

11. Proof was given by Chen and Mei that the stationarity of this functional is equivalent to the original boundary value problem.

12. The integral equation obtained from extremizing the functional is solved by using a finite-element method. This method is a technique of numerical approximation that involves dividing a domain into a number of nonoverlapping subdomains which are called elements.

13. The solution of the problem is approximated within each element by suitable interpolation functions in terms of a finite number of unknown parameters. These unknown parameters are the values of the field variable $\phi(x,y)$ at a finite number of points which are called nodes. The relations for individual elements are combined into a system of equations for all unknown parameters.

14. In the region outside the basin, the velocity potentials are solved analytically in terms of unknown coefficients. The region is considered a single element with an "interpolation function" given by Equation 3. The infinite series is terminated at a finite value such that the addition of further terms does not significantly influence the calculated values of $\phi(x,y)$. The resulting equation is combined with the system of equations for unknown parameters at nodal points within the basin and this complete system is solved using Gaussian elimination matrix methods.

15. $\eta(x,y)$ is related to $\phi(x,y)$ through the linearized dynamic free surface boundary condition

$$\eta(x,y) = - \frac{1}{g} \frac{\partial \phi(x,y)}{\partial t} \quad (6)$$

16. The horizontal velocity components have the following form:

$$u(x,y) = - \frac{g}{\omega} \frac{\partial \eta(x,y)}{\partial x}; \quad v(x,y) = - \frac{g}{\omega} \frac{\partial \eta(x,y)}{\partial y} \quad (7)$$

17. The hybrid finite-element method (so named by Chen and Mei because the method involves the combination of analytical and finite-element numerical solutions) is a steady-state solution of the boundary value problem. The steady-state response of a harbor to an arbitrary

forcing function can be easily determined within the framework of a linearized theory.

18. Plate 1 shows the finite-element grid used to portray East Channel and the surrounding harbor area. Grid modifications needed to represent the Federal project and the non-Federal dredging plans were easily accomplished by merely changing water depths in the dredged areas.

PART III: RESULTS

19. Wave-height amplification at a station inside the harbor is defined as the wave height at the station divided by twice the incident wave height. This definition of amplification factor is traditional and is a result of the fact that the standing wave height for a straight coast with no harbor (and total reflection) would be twice the incident wave height due to superposition of incident and reflected waves. Wave-height amplification for all plans at sta 1 (north end of East Channel) over the 60- to 600-sec period range is illustrated in Plates 2-5. Station locations are shown in Figure 6. Normalized maximum current

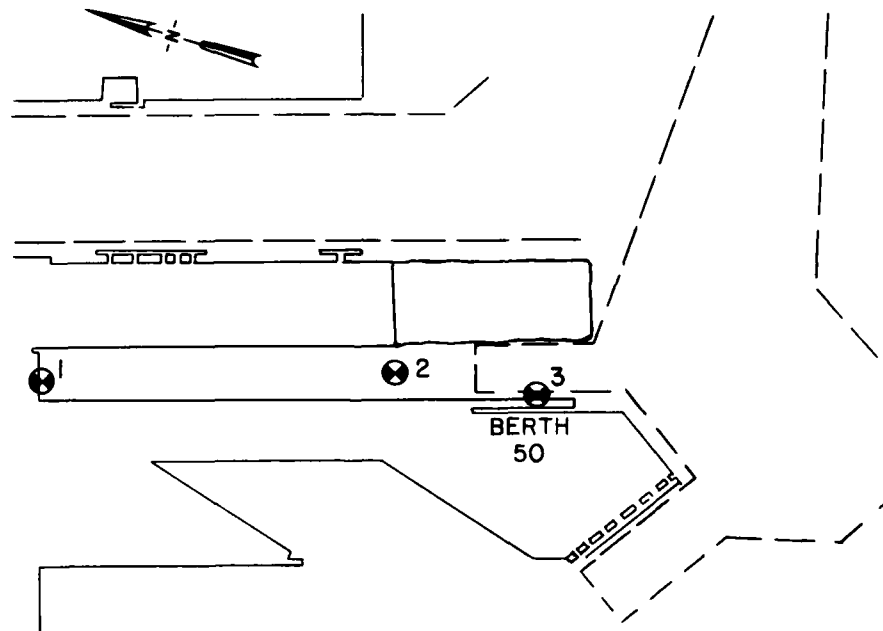


Figure 6. Station locations

velocity (NMCV) as a function of wave period is shown in Plates 6-9 for sta 2 (entrance to East Channel). The plotted current velocity multiplied by the incident wave height in feet (or metres) gives velocity in units of feet per second (or metres per second). The computed velocities have no vertical component or variation since linear long-wave theory is used. The velocity plotted is the maximum that would occur over a wave period.

NMCV results for sta 3 (berth 50, Bulk Loading Terminal) are shown in Plates 10-13.

20. Plates 2-5 show that the calculated amplification at sta 1 in East Channel for the base plan was less than 4 over the 60- to 600-sec period range with the exception of the fundamental mode of oscillation centered at 360.5 sec. Resonant response in the 60- to 200-sec period range consisted of lower, relatively broad peaks centered at 66, 92, 106, and 134 sec. The resonant response for the Phase I-B, I-B w/NFD-1, and I-B w/NFD-2 plans was similar to the base plan at periods less than the fundamental mode of oscillation except for some shifts in central frequency of the peak response. For the fundamental mode of oscillation near 360 sec, significant differences in the amplification magnitude occurred. Central periods (T) and amplitudes of maximum wave-height amplification (R) for the base plan and the three harbor improvement plans were:

Base		Phase I-B		Phase I-B w/NFD-1		Phase I-B w/NFD-2	
T, sec	R	T, sec	R	T, sec	R	T, sec	R
66.0	2.7	66.0	2.9	66.0	2.9	66.0	3.0
92.0	2.6	92.0	2.4	92.0	2.2	92.0	2.2
106.0	3.0	106.0	2.9	106.0	2.4	106.0	2.7
134.0	3.6	128.0	4.2	118.0	3.9	127.0	4.2
360.5	45.4	353.0	34.2	334.5	76.5	348.0	42.2

Amplification for modes of oscillation at periods less than that of the fundamental mode was generally broad and not sharply peaked. Amplification for the fundamental mode was sharply peaked for all plans. However, the bandwidth of the resonant mode decreased for the Phase I-B w/NFD-1 plan which had significantly increased amplification. The bandwidth for each plan of the resonant amplification for the fundamental mode at a level equal to 25 percent of the maximum amplification was:

Plan	Period sec	Peak Amplification	25 Percent Amplification Level	Bandwidth sec
Base	360.5	45.4	11.4	13
Phase I-B	353.0	34.2	8.6	9

(Continued)

Plan	Period sec	Peak Amplification	25 Percent Amplification Level	Bandwidth sec
Phase I-B w/NFD-1	334.5	76.5	19.1	2
Phase I-B w/NFD-2	348.0	42.2	10.6	9

21. NMCV data for the entrance to East Channel (Plates 6-9) show a trend similar to amplification data for the north end of the channel. Peak normalized currents at sta 2 again occurred at the same periods as maximum amplification at sta 1 except for the base plan where the period for the NMCV shifted from 66.0 to 64.0 sec. Also, the amplification peak for the base plan at 134.0 sec was not clearly defined in the NMCV data and had shifted to 128 sec. Central periods and magnitudes of the NMCV at sta 2 for each plan were:

Base		Phase I-B		Phase I-B w/NFD-1		Phase I-B w/NFD-2	
T, sec	NMVC	T, sec	NMCV	T, sec	NMCV	T, sec	NMCV
64.0	3.5	66.0	3.0	66.0	2.5	66.0	3.0
92.0	3.1	92.0	3.2	92.0	2.5	92.0	2.9
106.0	4.1	106.0	4.1	106.0	2.9	106.0	2.7
128.0	2.3	128.0	2.7	118.0	3.3	127.0	3.3
360.5	57.1	353.0	46.0	334.5	85.0	348.0	57.3

The NMCV data for fundamental modes of oscillation for each plan were significantly larger in magnitude than for the shorter period oscillations.

22. For periods less than 200 sec, NMCV at sta 3 adjacent to berth 50 (Plates 10-13) peaked for each plan between 120 and 140 sec with smaller peaks between 60 and 100 sec. The maximum NMCV at sta 3 for each plan again occurred at the period of the fundamental oscillation of East Channel. For the fundamental oscillations, the NMCV was highest for the base plan and smallest for the Phase I-B w/NFD-2 plan. The NMCV for the NFD-1 plan at berth 50 for the fundamental oscillation was smaller than for the base plan although the wave-height amplification of the NFD-1 plan was largest for sta 1 in East Channel. The decreased velocity for the NFD-1 plan relative to the base plan shows the influence of the

outer harbor area and the plan modification on the fundamental model of oscillation for the channel. Central periods and magnitudes of the NMCV at sta 3 for each plan were:

Base		Phase I-B		Phase I-B w/NFD-1		Phase I-B w/NFD-2	
T, sec	NMCV	T, sec	NMCV	T, sec	NMCV	T, sec	NMCV
63.0	1.7	63.0	1.5	--	--	--	--
83.5	2.4	80.0	2.0	80.0	2.1	81.0	2.2
92.5	2.1	88.0	2.0	87.0	2.0	88.0	2.2
134.0	3.7	132.0	3.8	124.0	2.4	129.0	3.0
--	--	--	--	140.0	2.4	--	--
360.0	21.2	353.0	13.9	334.5	17.0	347.5	11.5

23. Contours of wave-height amplification and NMCV vectors for the 66-, 92-, 106-, 134-, and 360.5-sec modes of oscillation for the base plan are shown in Plates 14-23. Locations of nodes and antinodes in the modes of oscillation can easily be seen in the plots. In the base plan the 66.0-sec oscillation had antinodes at the north end of the channel, at the center, and just inside the entrance (Plate 14). The 92.0-sec mode had antinodes at the north end of the channel and at a location approximately 40 percent of the channel length from the entrance, with the node slightly inside the entrance (Plate 16). The 106.0-sec mode had antinodes at the north end and at a location approximately 25 percent of the channel length from the entrance (Plate 18). The node for the 106.0-sec mode was located at the channel entrance. The 134.0-sec mode had antinodes at the north end of the channel and slightly inside the channel entrance (Plate 20). The fundamental mode of oscillation at 360.5 sec developed with the node near berth 50 and an antinode at the north end of the channel (Plate 22).

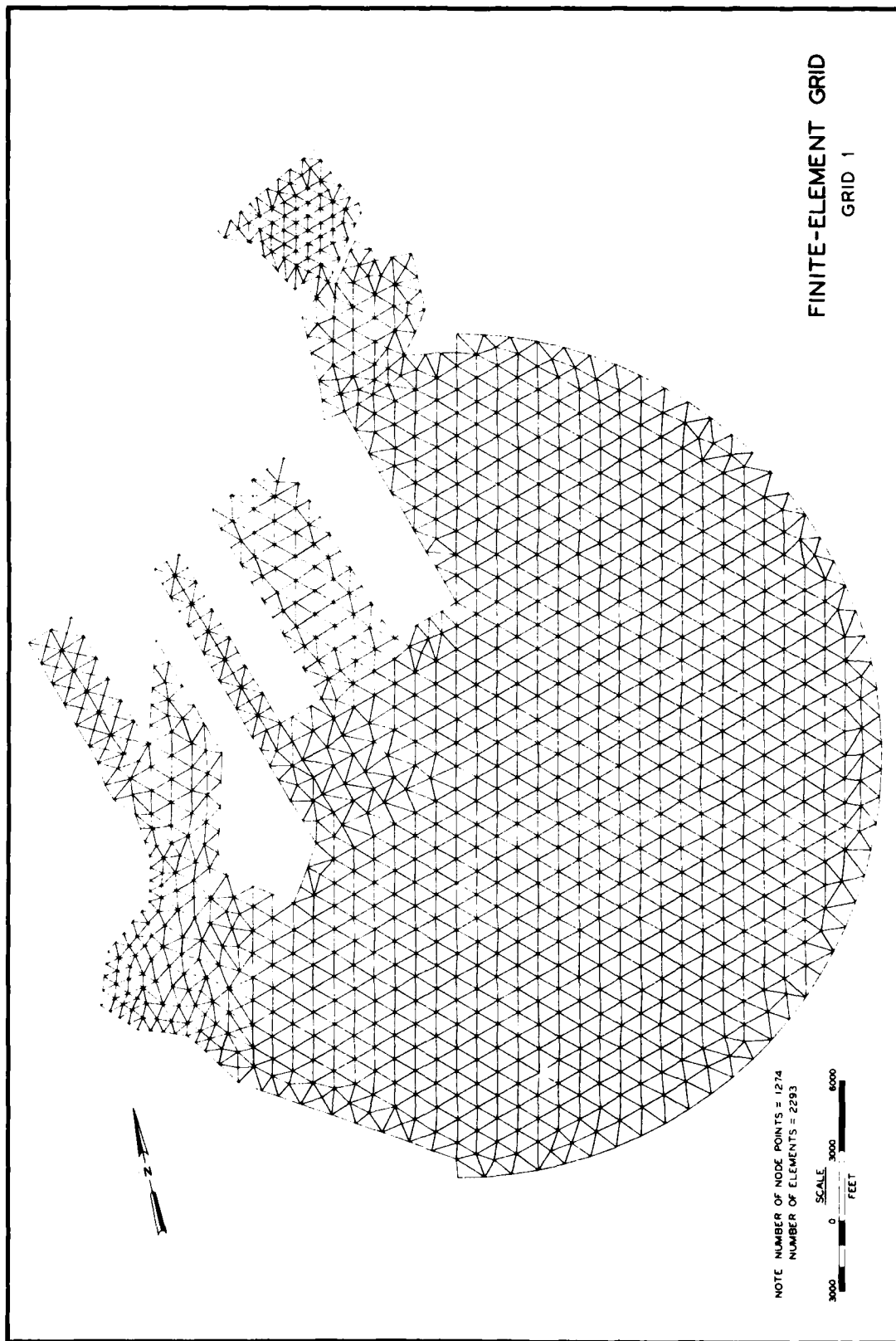
24. Modes of oscillation for the base plan and the three improvement plans considered were quite similar at periods less than the fundamental period of oscillation. The fundamental modes, however, are significantly different in amplification, period, and half-width of maximum response. Contours of wave-height amplification and the NMCV vectors for each of the fundamental modes with each of the three plans are shown in Plates 24-29. The midpoint of the NMCV vectors represent the point at

which the magnitudes were computed (Plates 15, 17, 19, 21, 23, 25, 27, and 29). In each plan, the peak NMCV for the fundamental mode occurred at the region of maximum rate of change in surface slope or just inside the channel entrance.

PART IV: CONCLUSIONS

25. Comparison of relative wave-height amplification and NMCV data for East Channel of the Port of Los Angeles for the base plan and three proposed improvement plans indicates relatively small differences in maximum amplification and maximum currents during resonant oscillations below 200 sec. Channel response varied significantly for the fundamental mode of oscillation (about 330-360 sec) for each plan. Wave-height amplification for the fundamental mode at the closed (north) end of East Channel increased 69 percent relative to the base plan for improvement plan Phase I-B w/NFD-1 and was a minimum for improvement plan Phase I-B (25 percent decrease relative to the base plan). Wave-height amplification for improvement plan Phase I-B w/NFD-2 was decreased 7 percent relative to the base plan.

26. It can be inferred that for the Phase I-B plan where the peak response for the fundamental mode decreased 25 percent and response for shorter period resonant oscillations was not significantly changed, mooring conditions, if changed, should improve. Phase I-B w/NFD-2 plan results were similar to base plan results except for the shift in period of the fundamental mode of oscillation (360.5 to 348.0 sec); consequently, mooring conditions should be similar to those for the base plan. The increase in amplification of the fundamental mode of oscillation for improvement plan Phase I-B w/NFD-1 could have an adverse impact on mooring conditions if the moored ship exhibited a resonant response at the same frequency.



FINITE-ELEMENT GRID
GRID 1

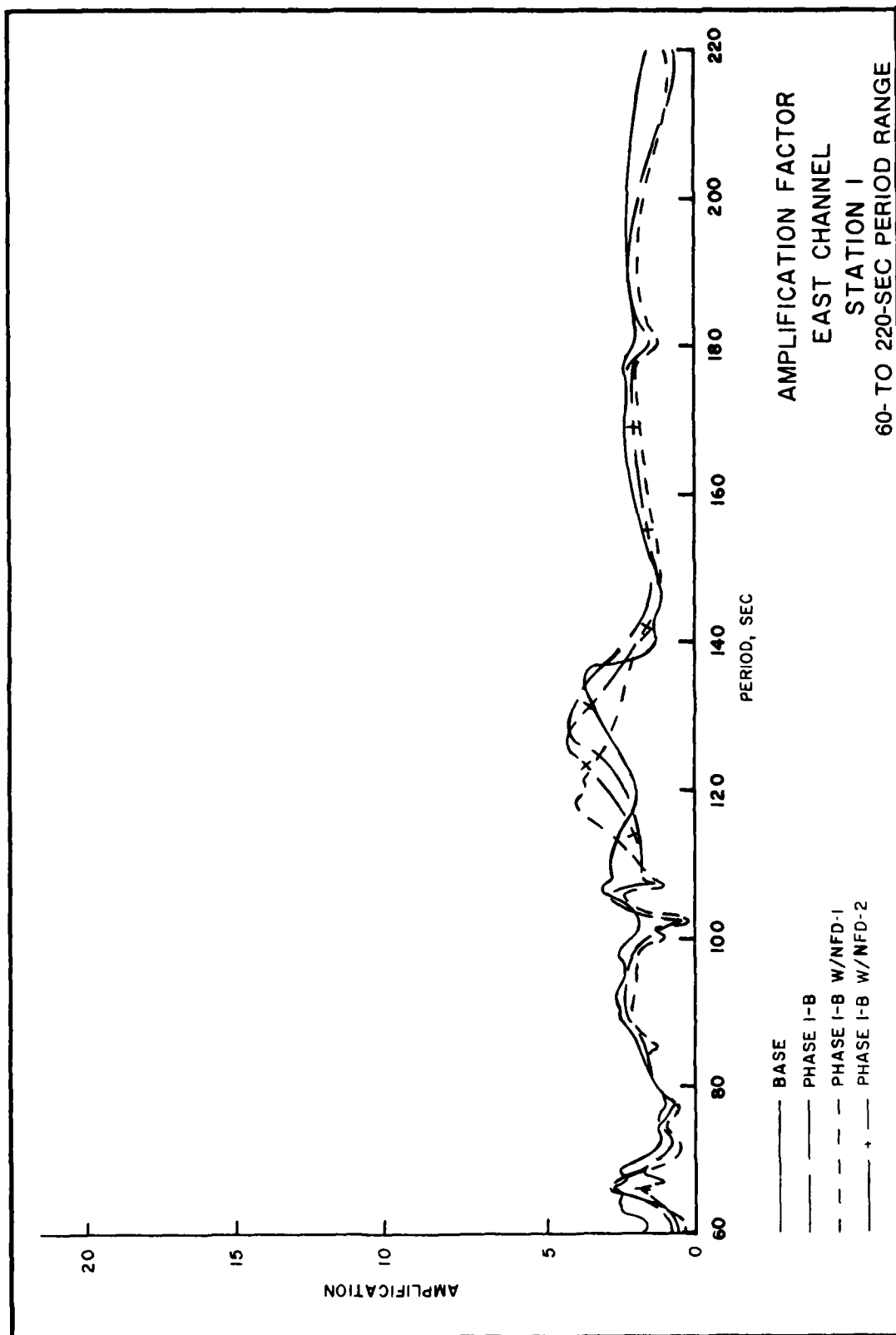
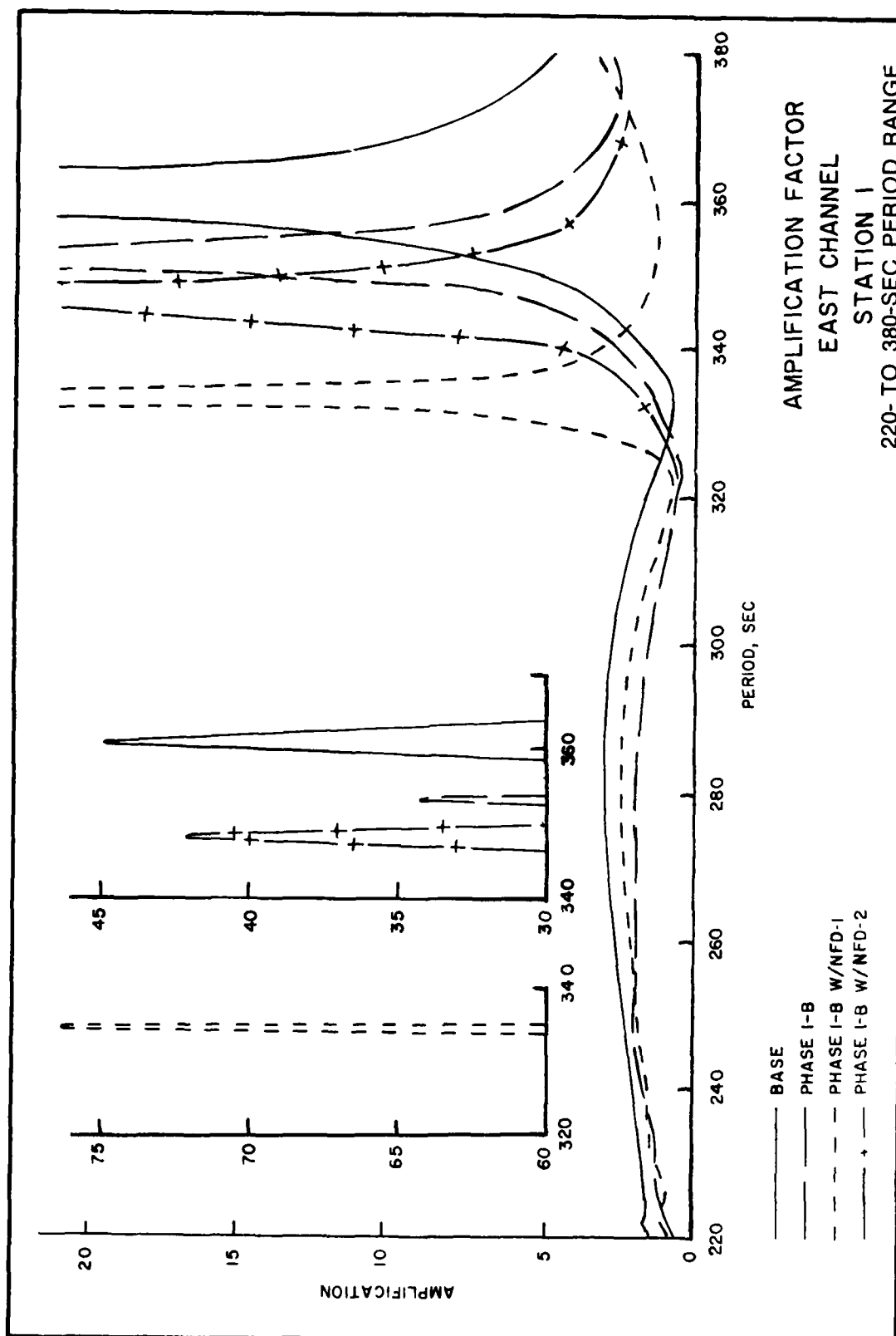


PLATE 2



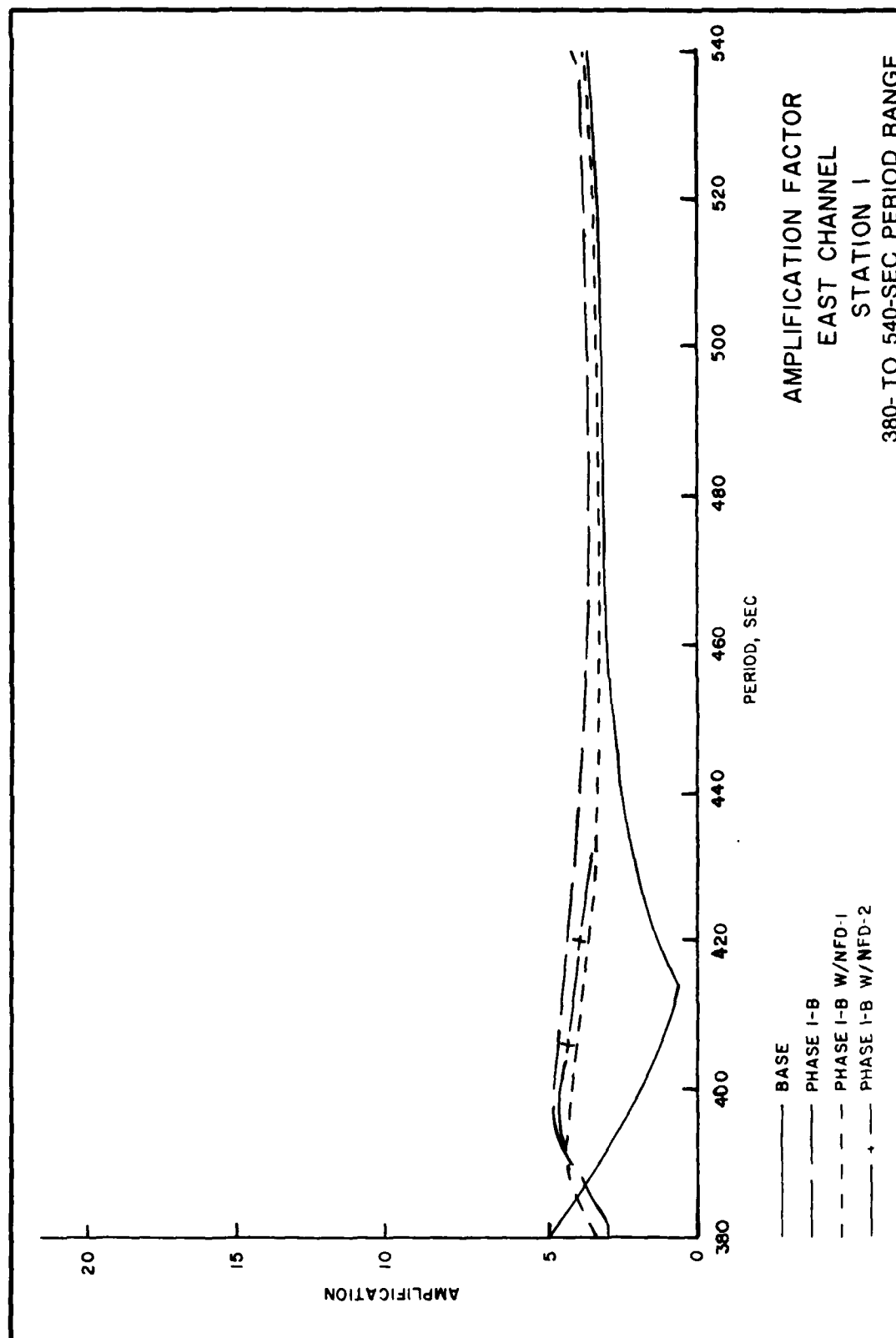
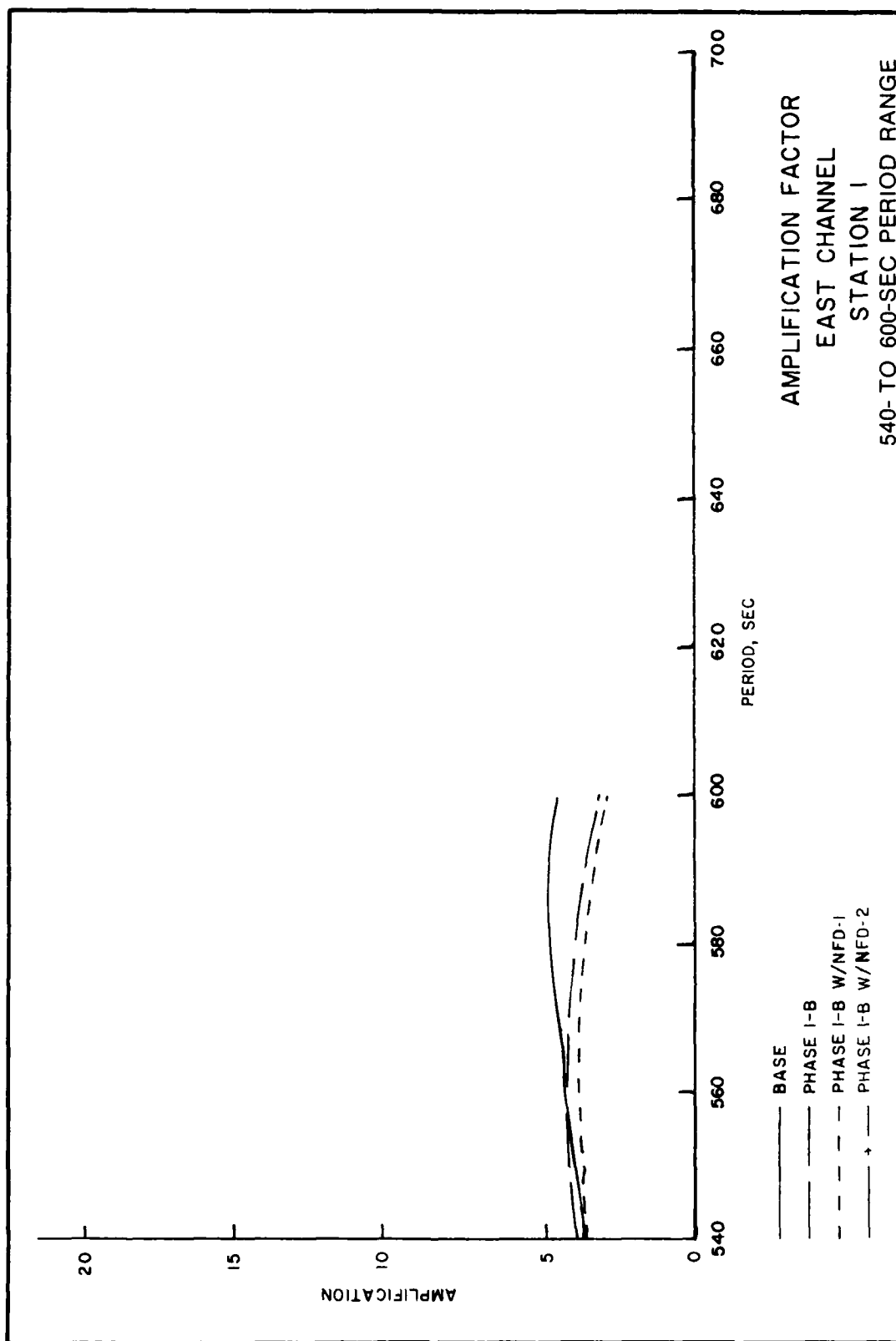


PLATE 4



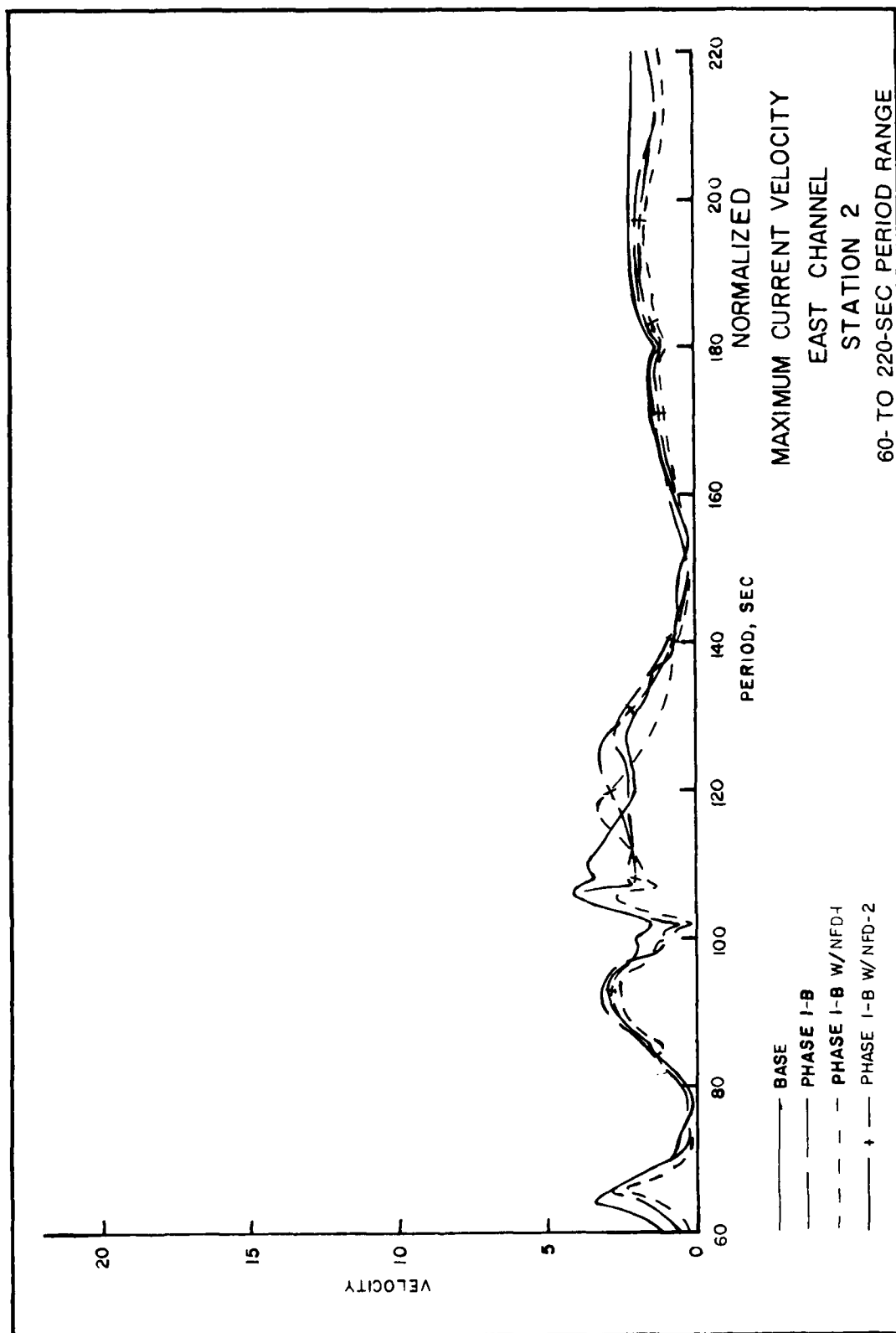
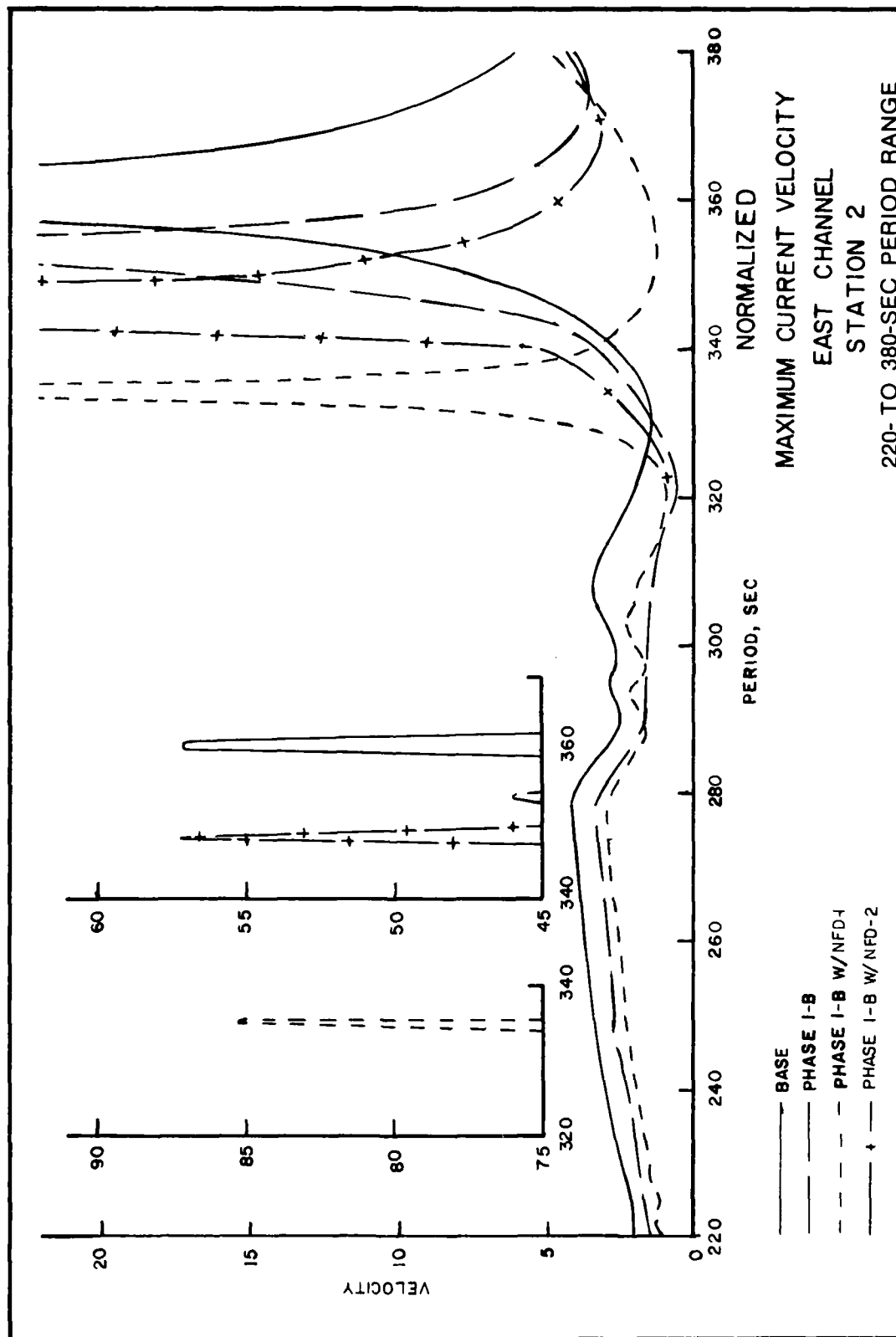


PLATE 6



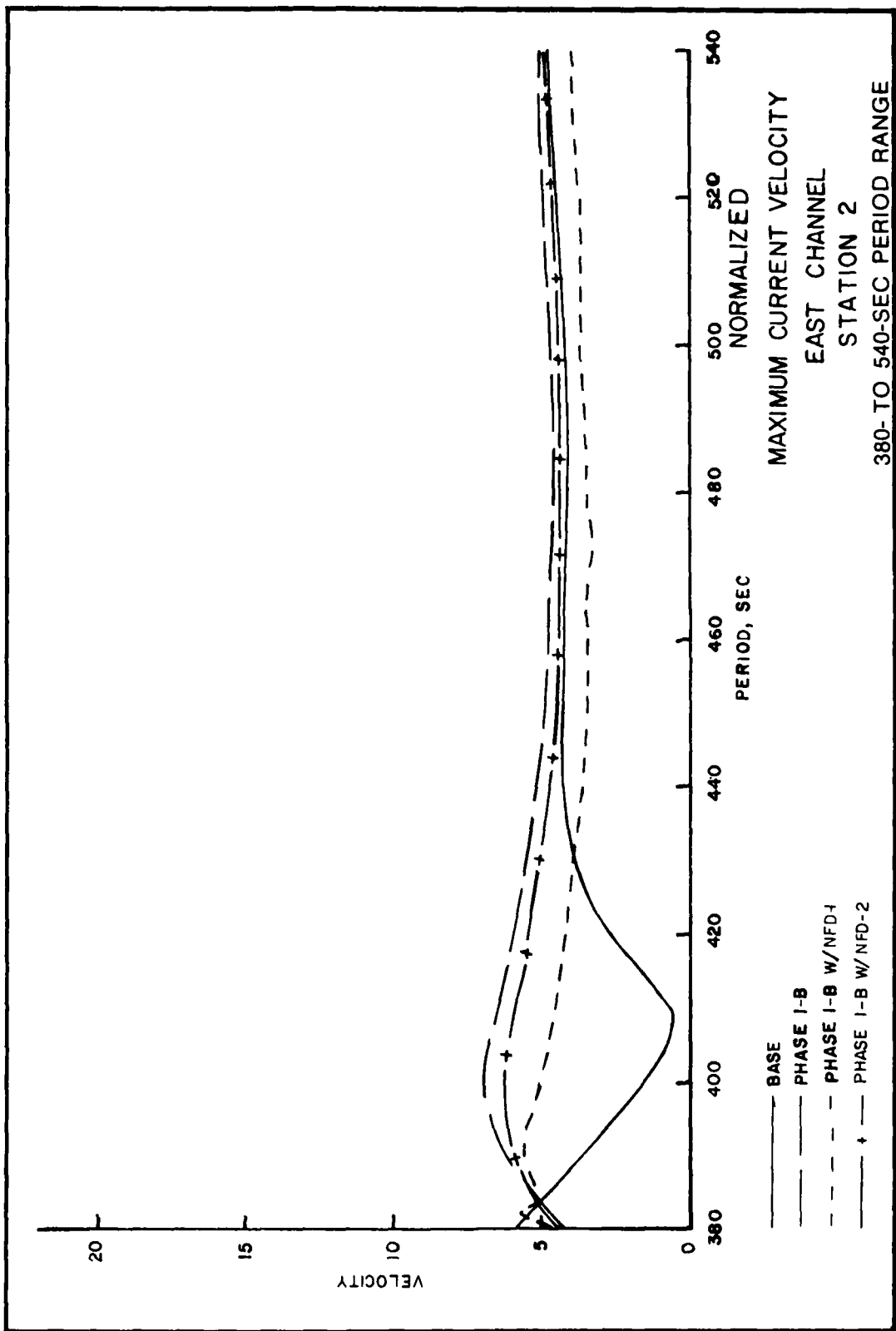


PLATE 8

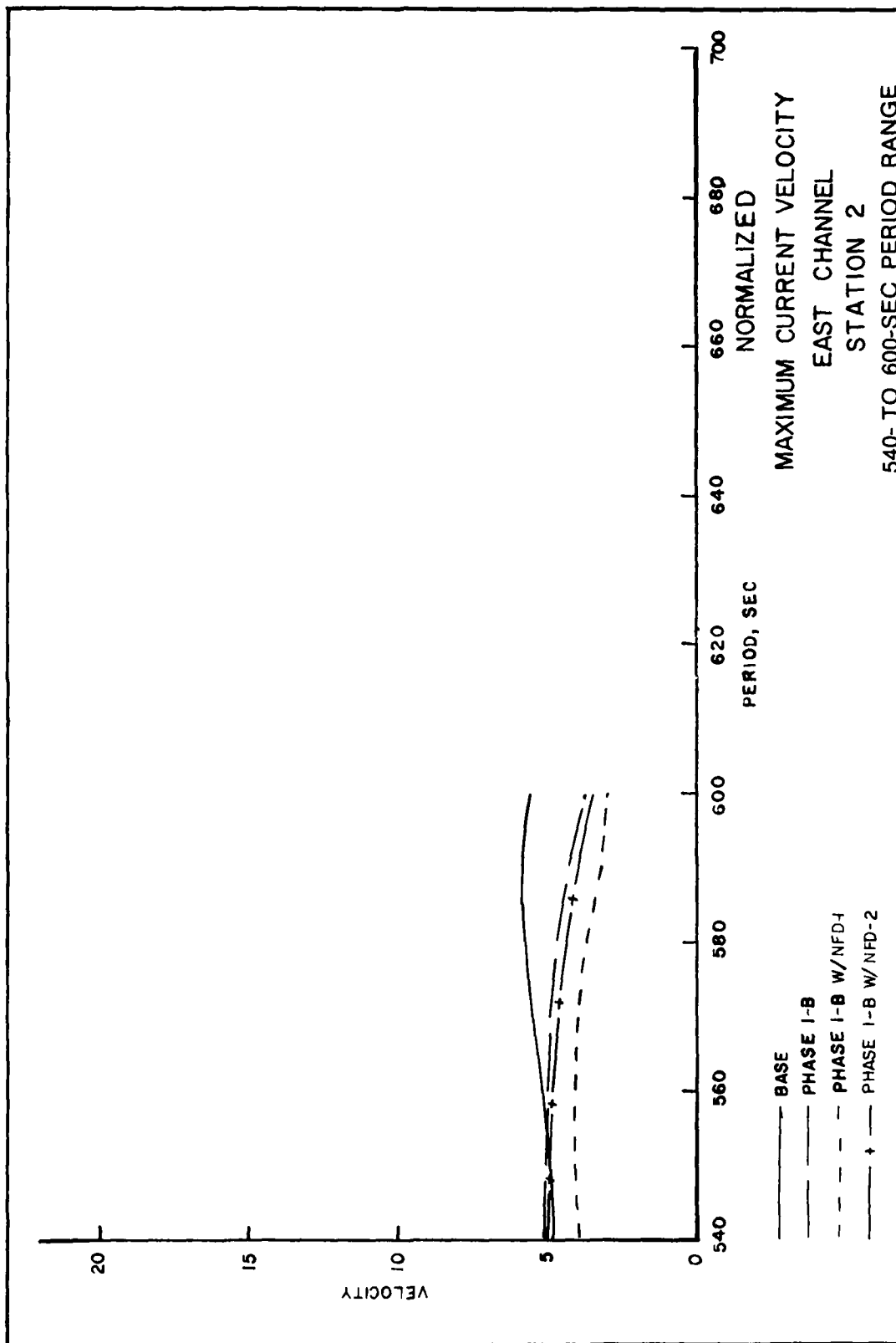


PLATE 9

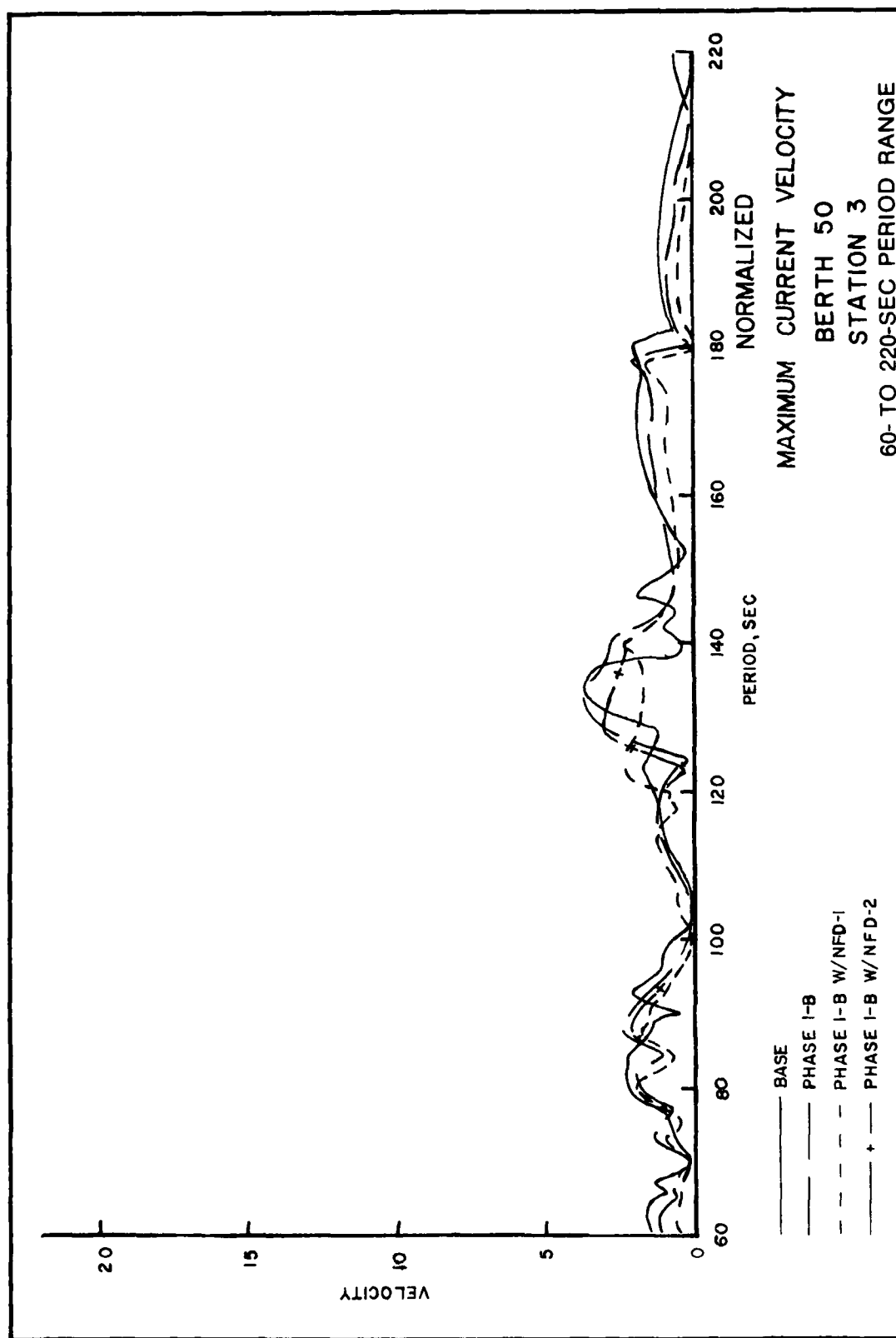
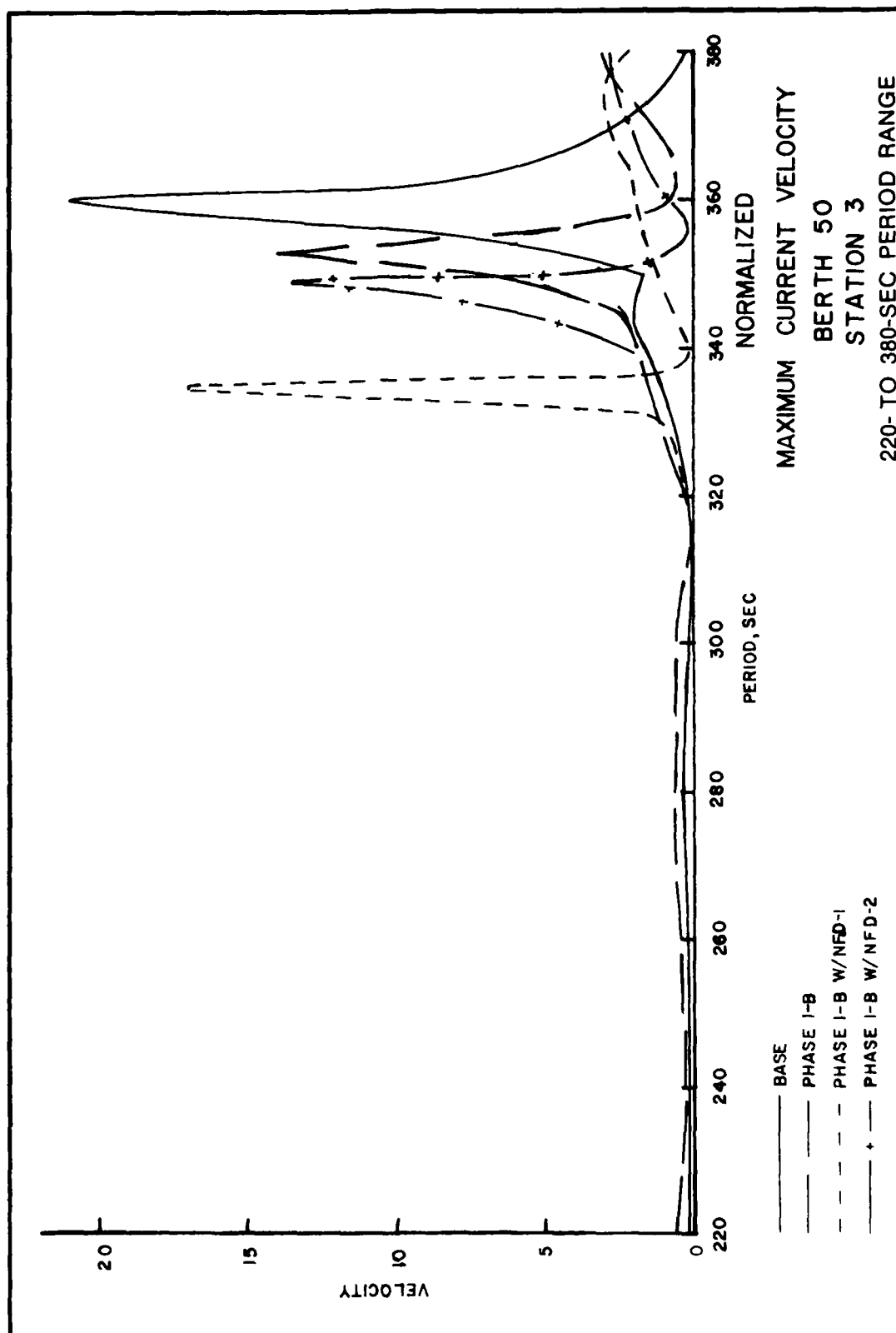


PLATE 10



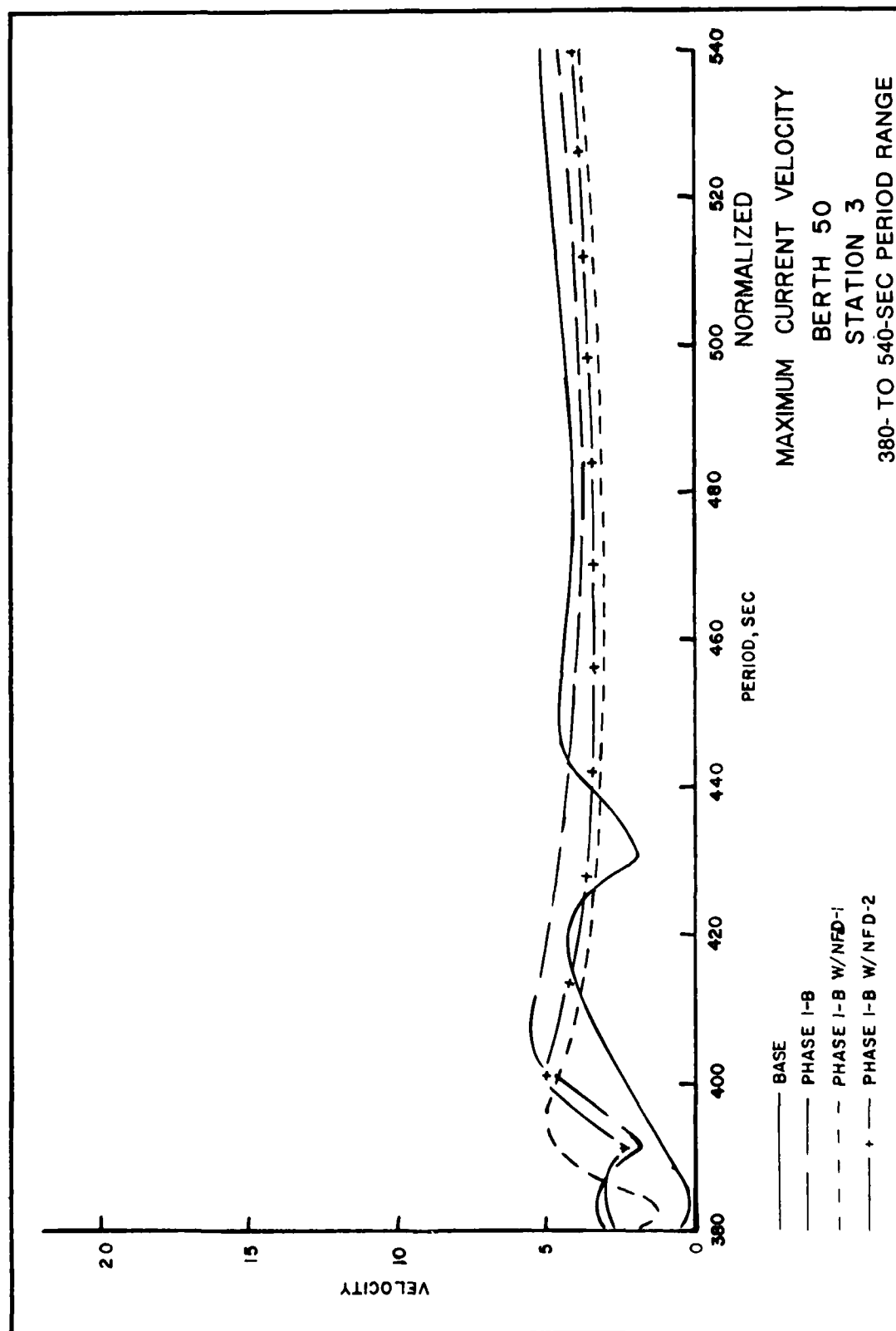


PLATE 12

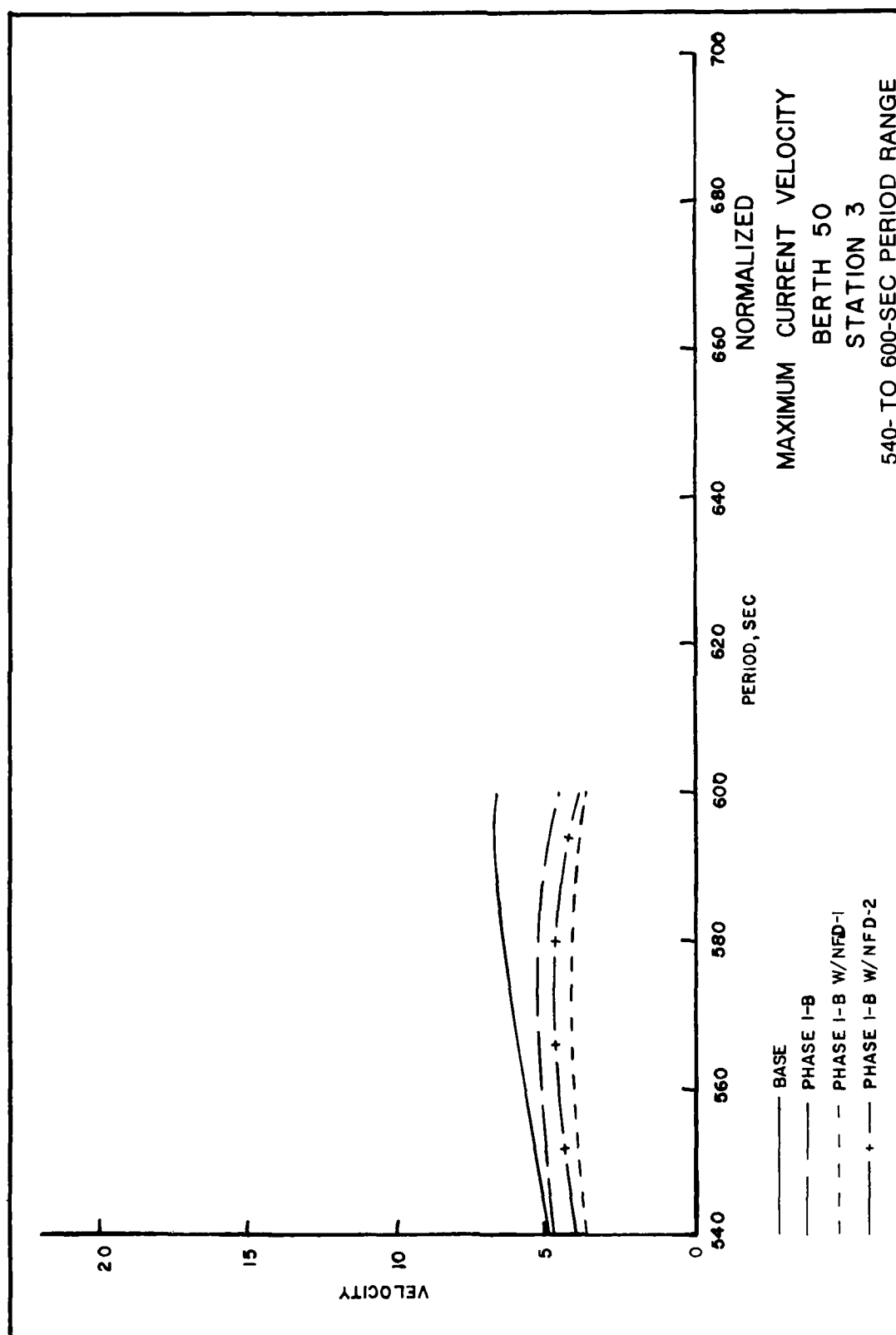


PLATE 13

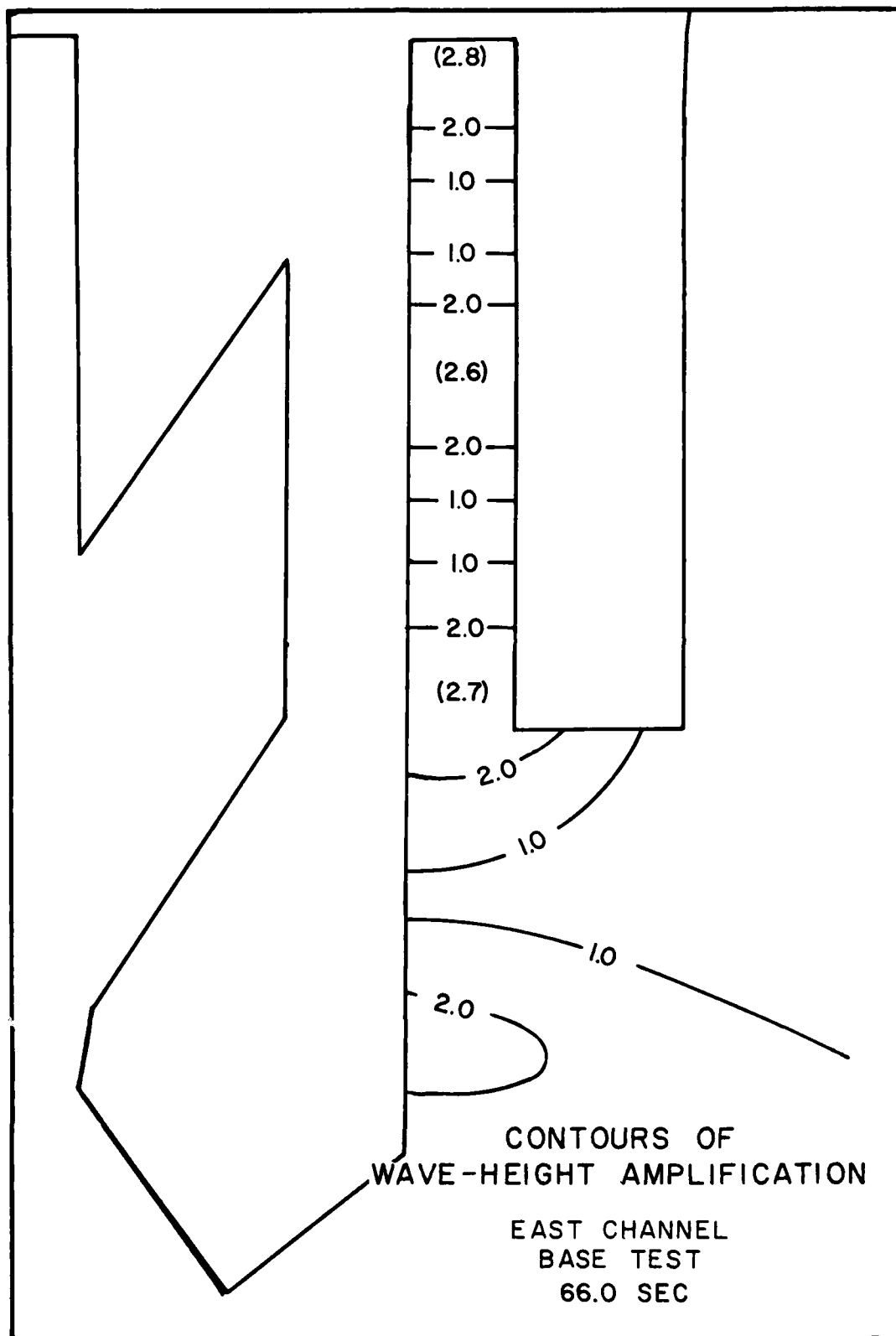
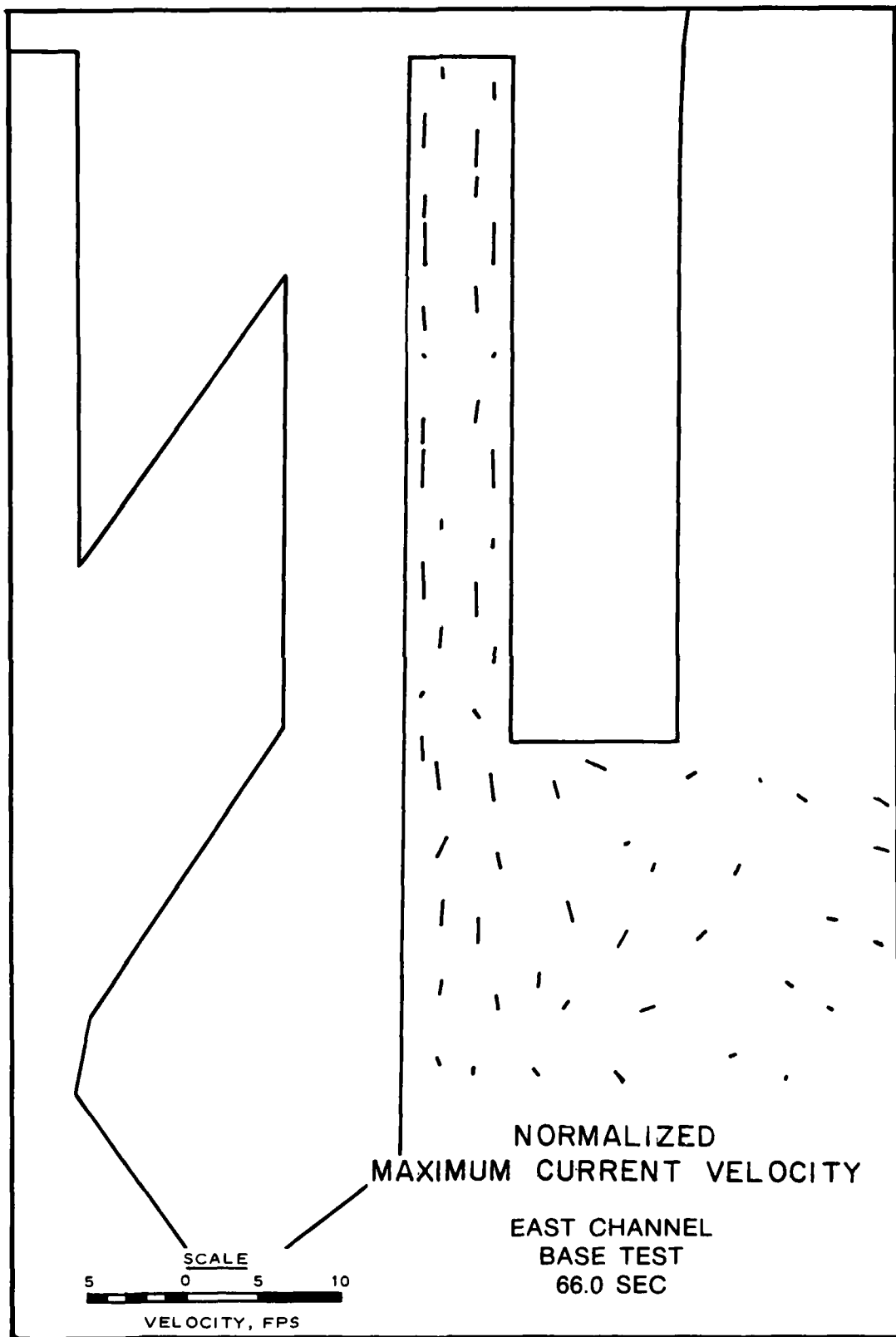


PLATE 14



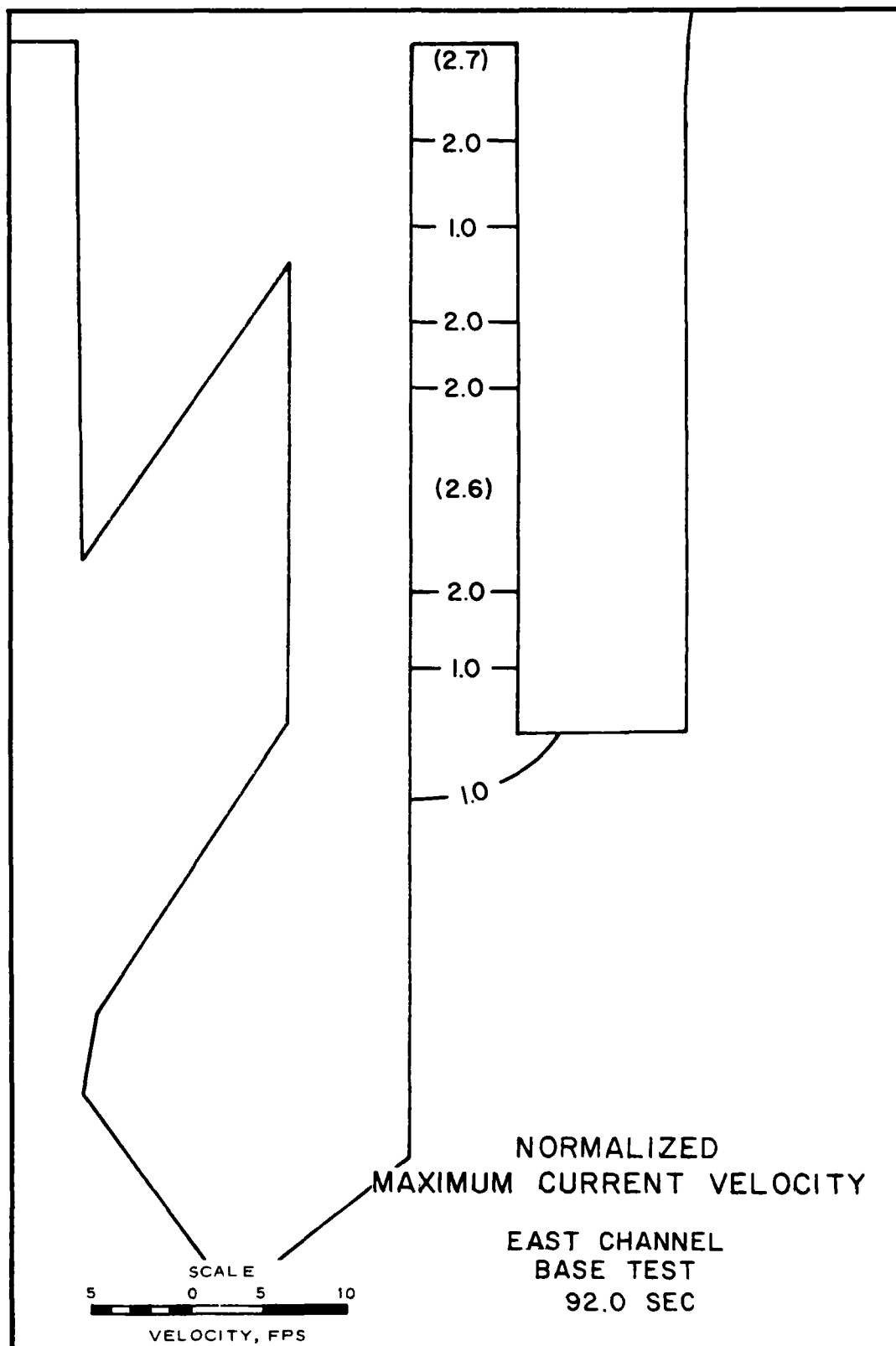
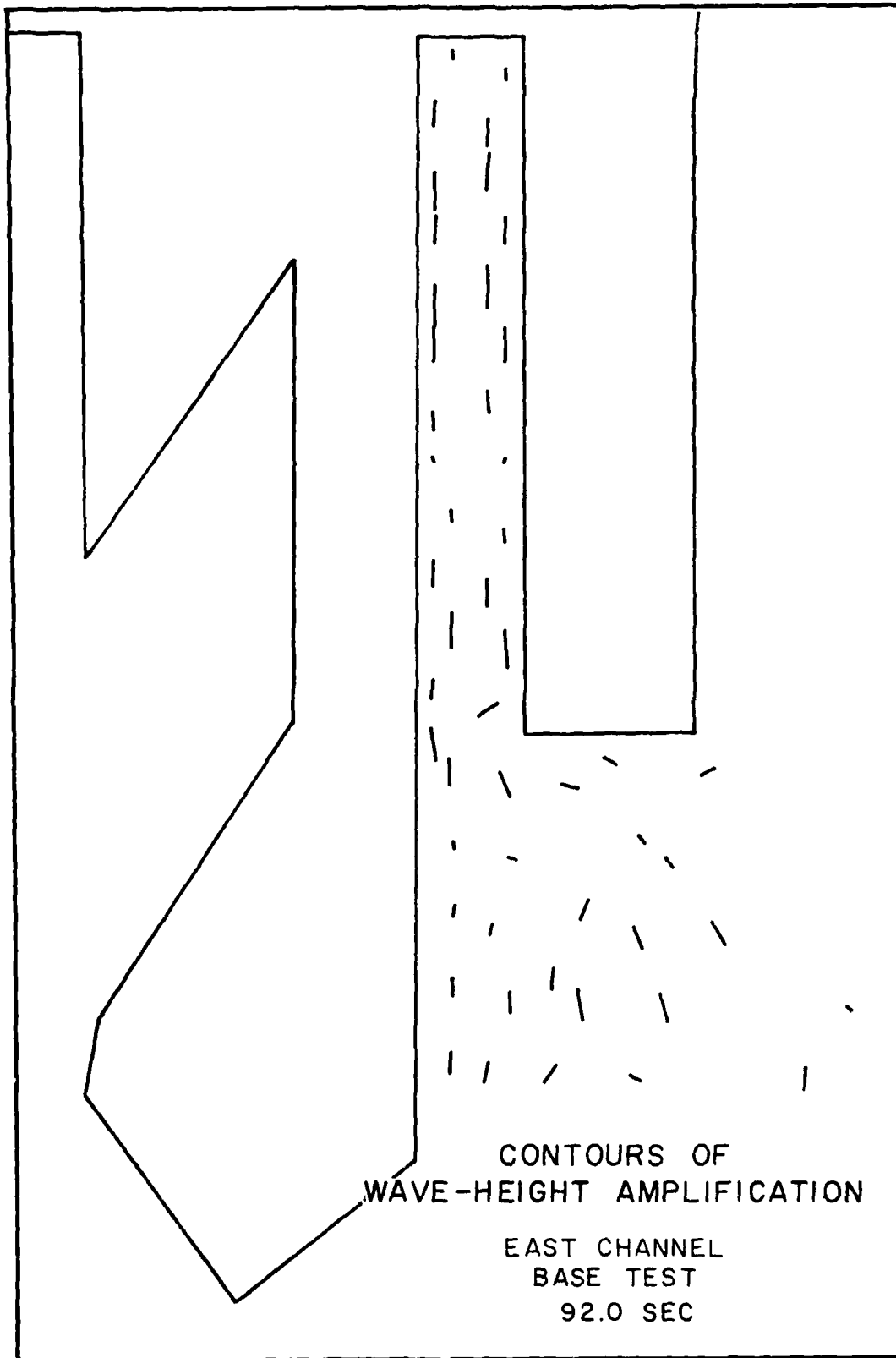
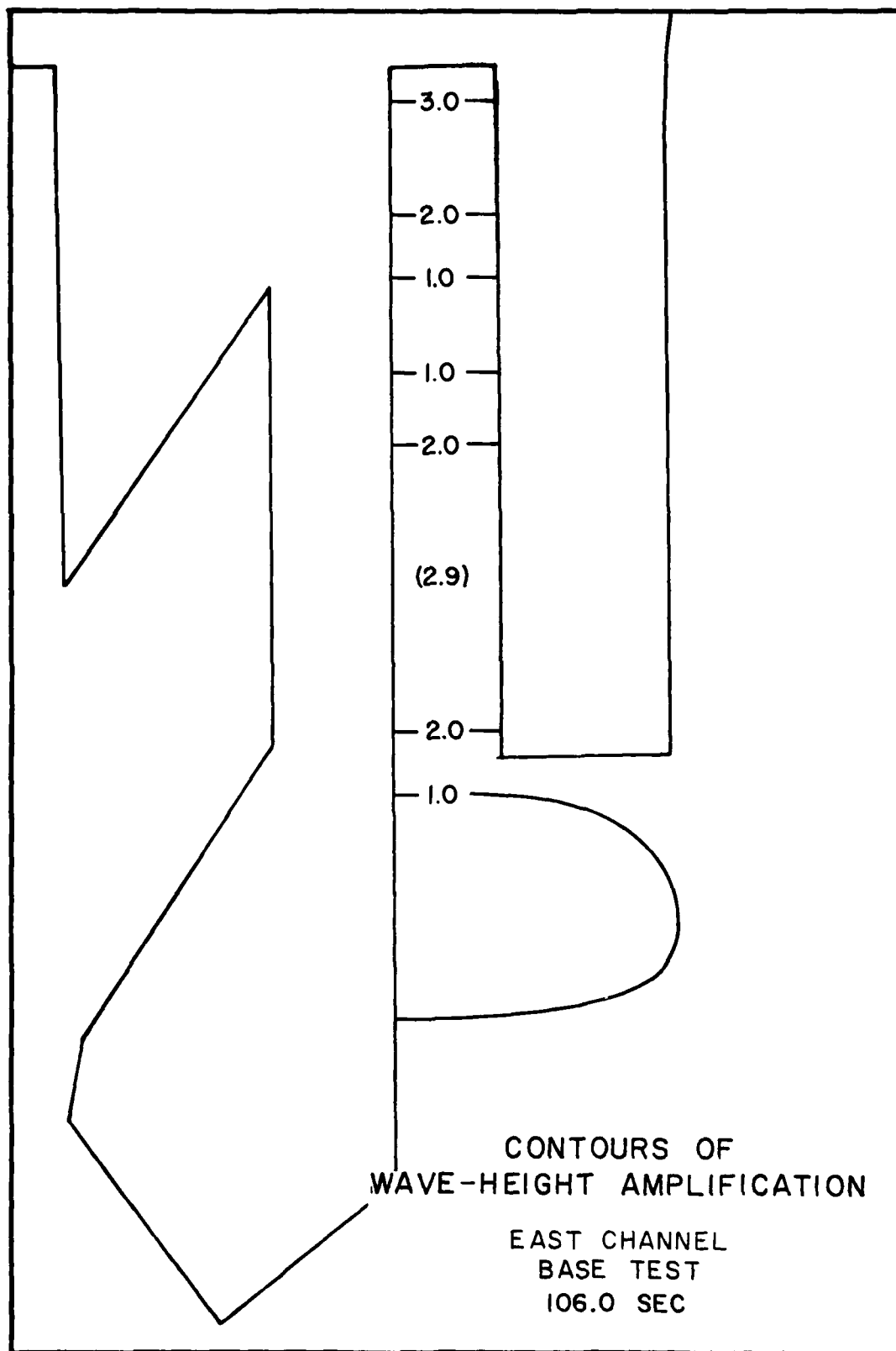
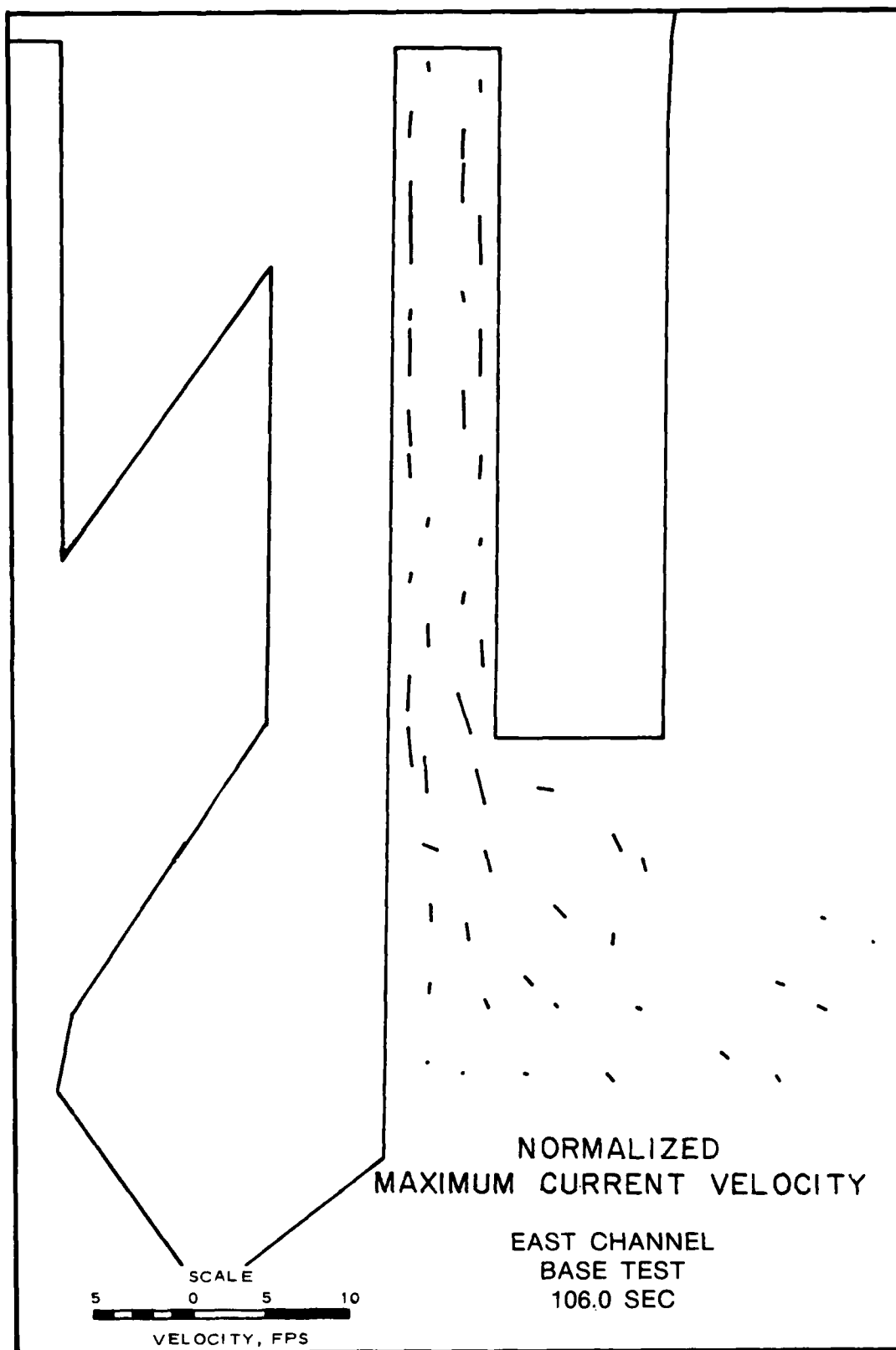
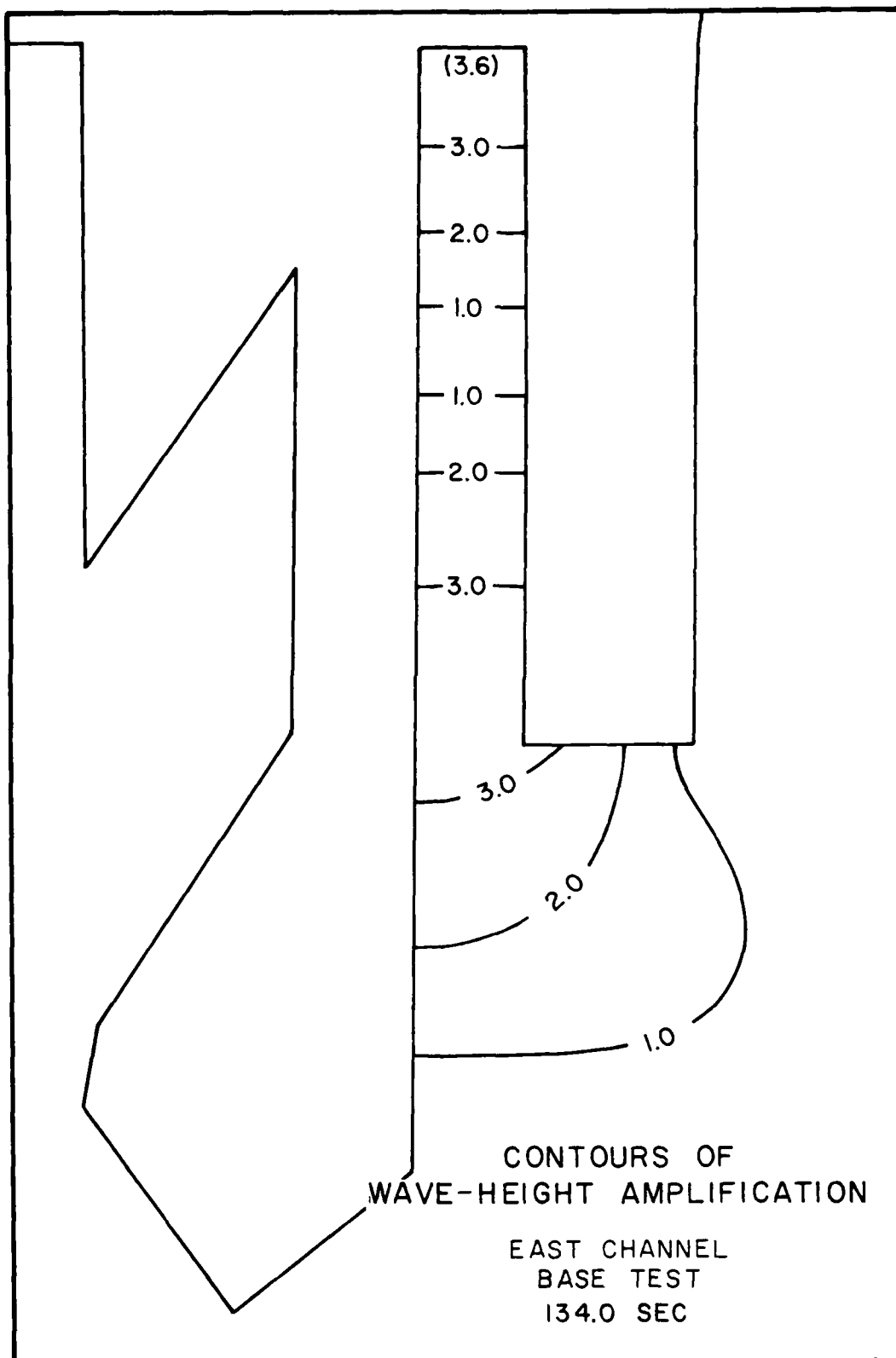


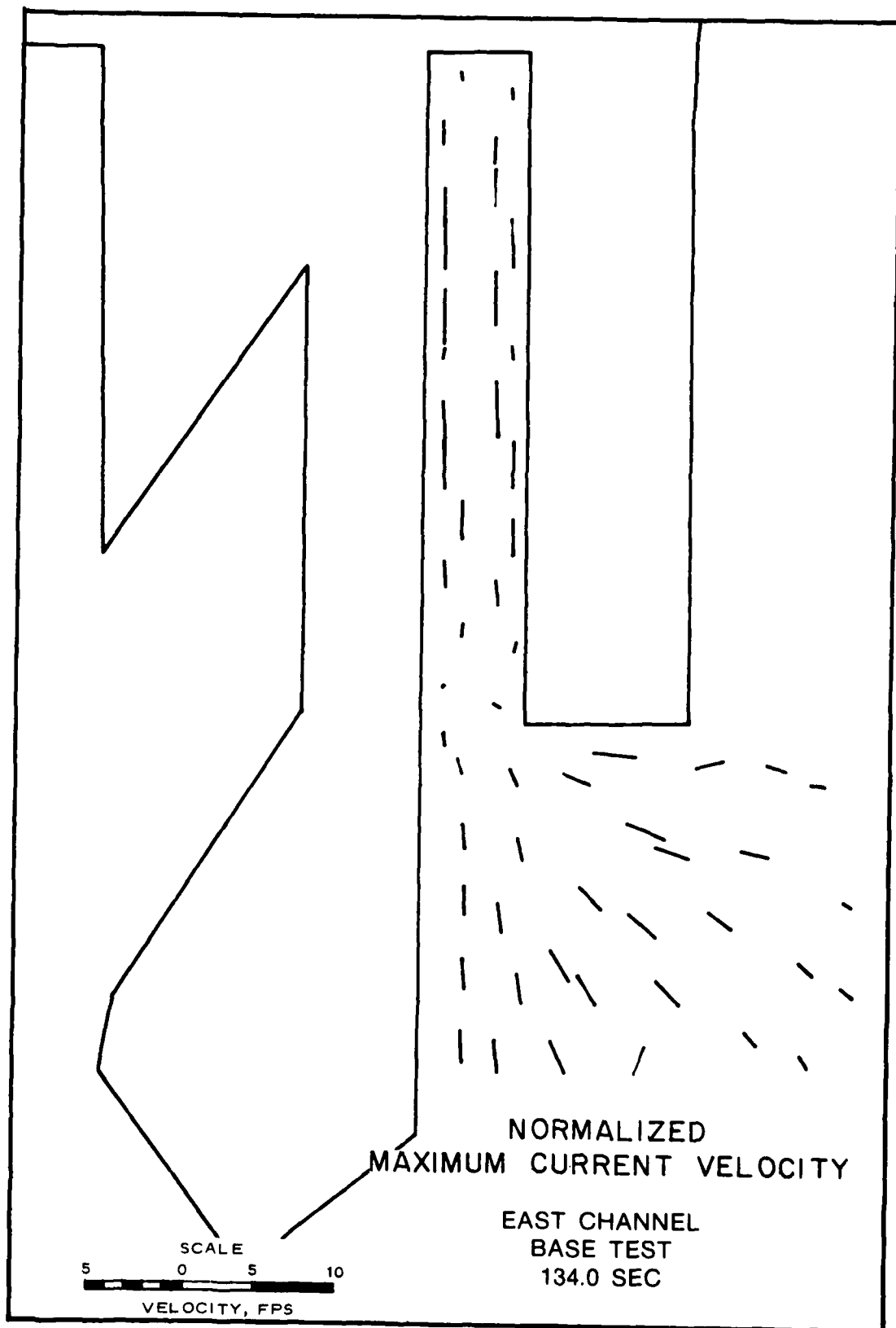
PLATE 16

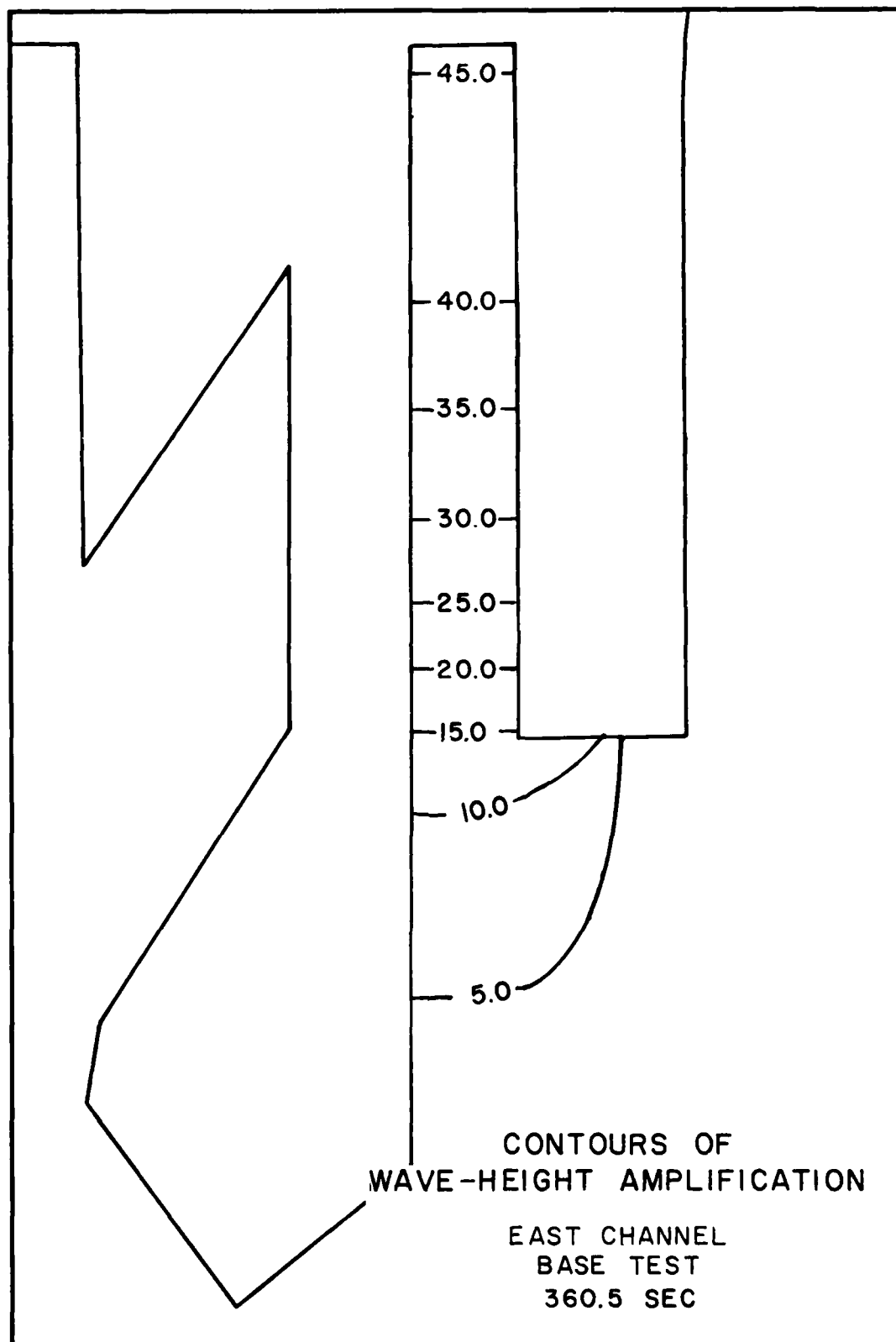


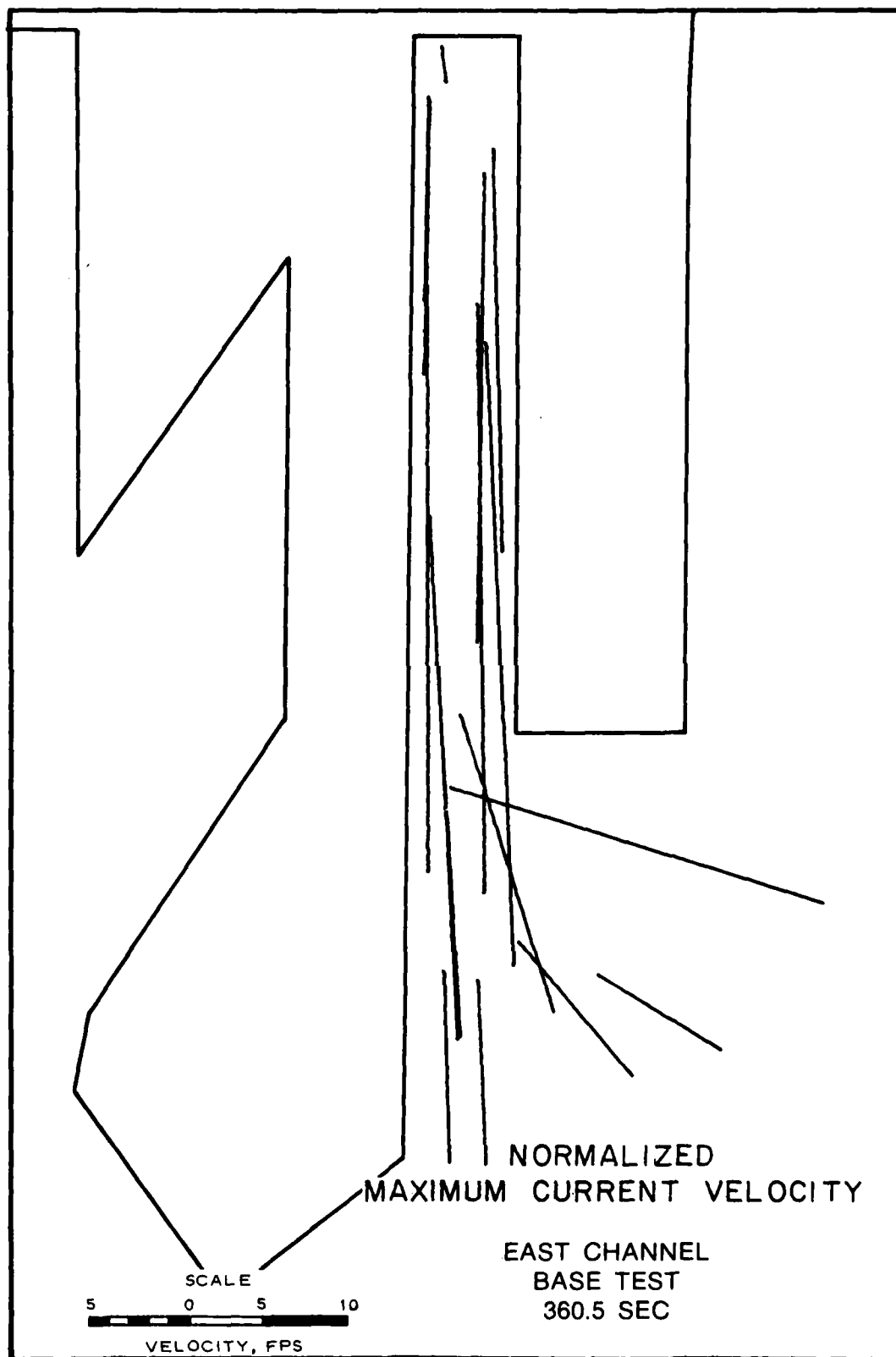


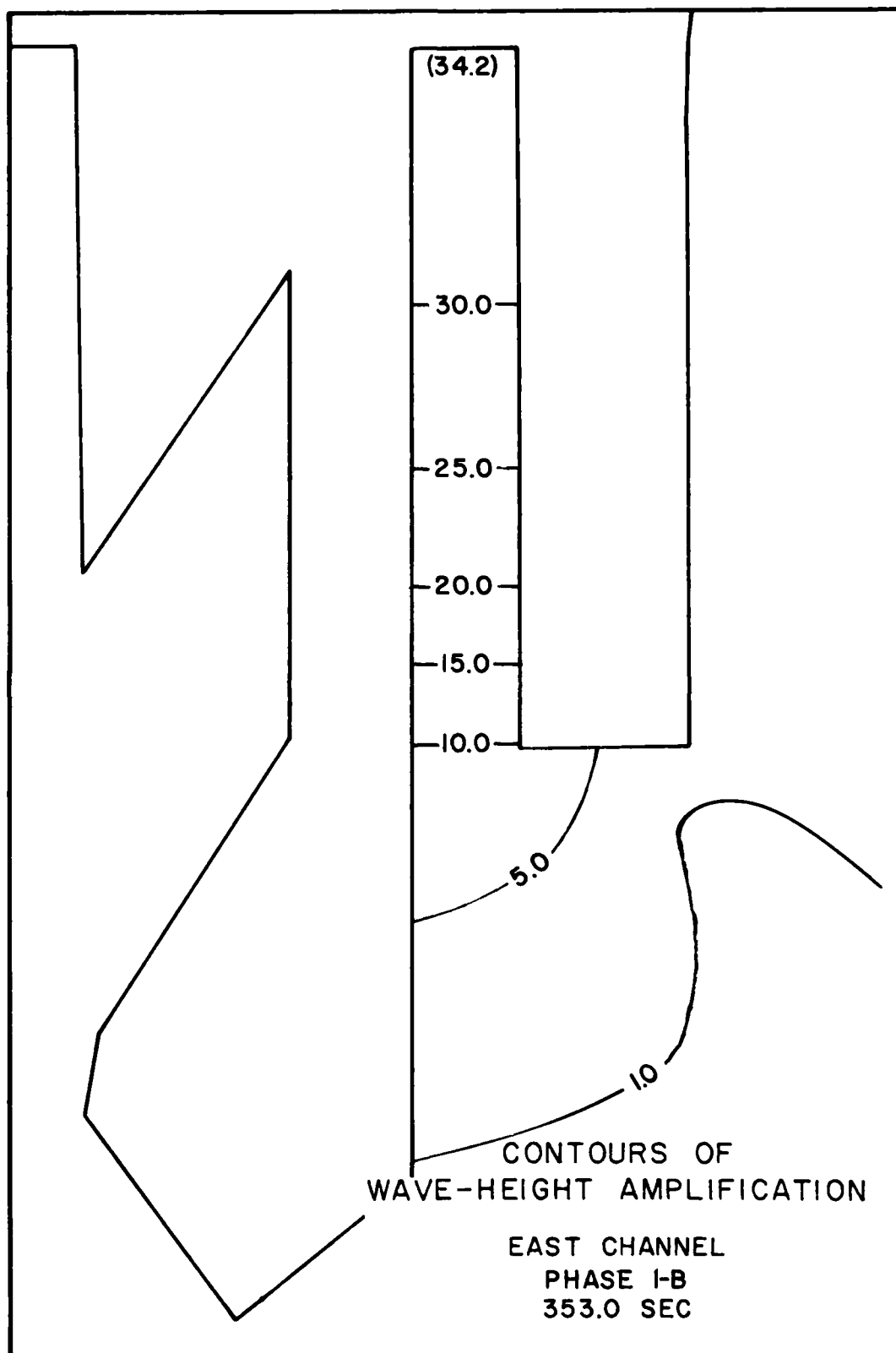


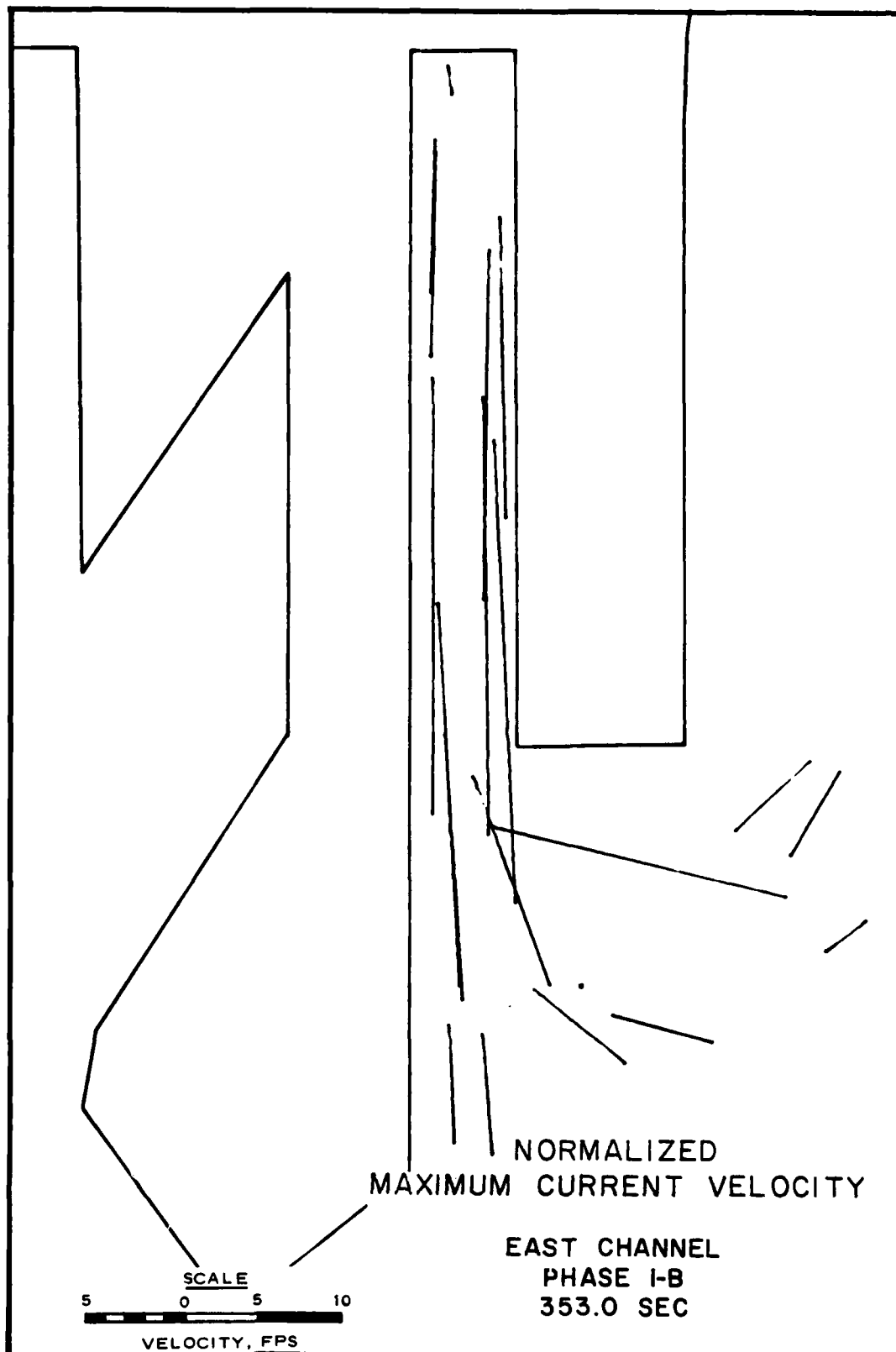












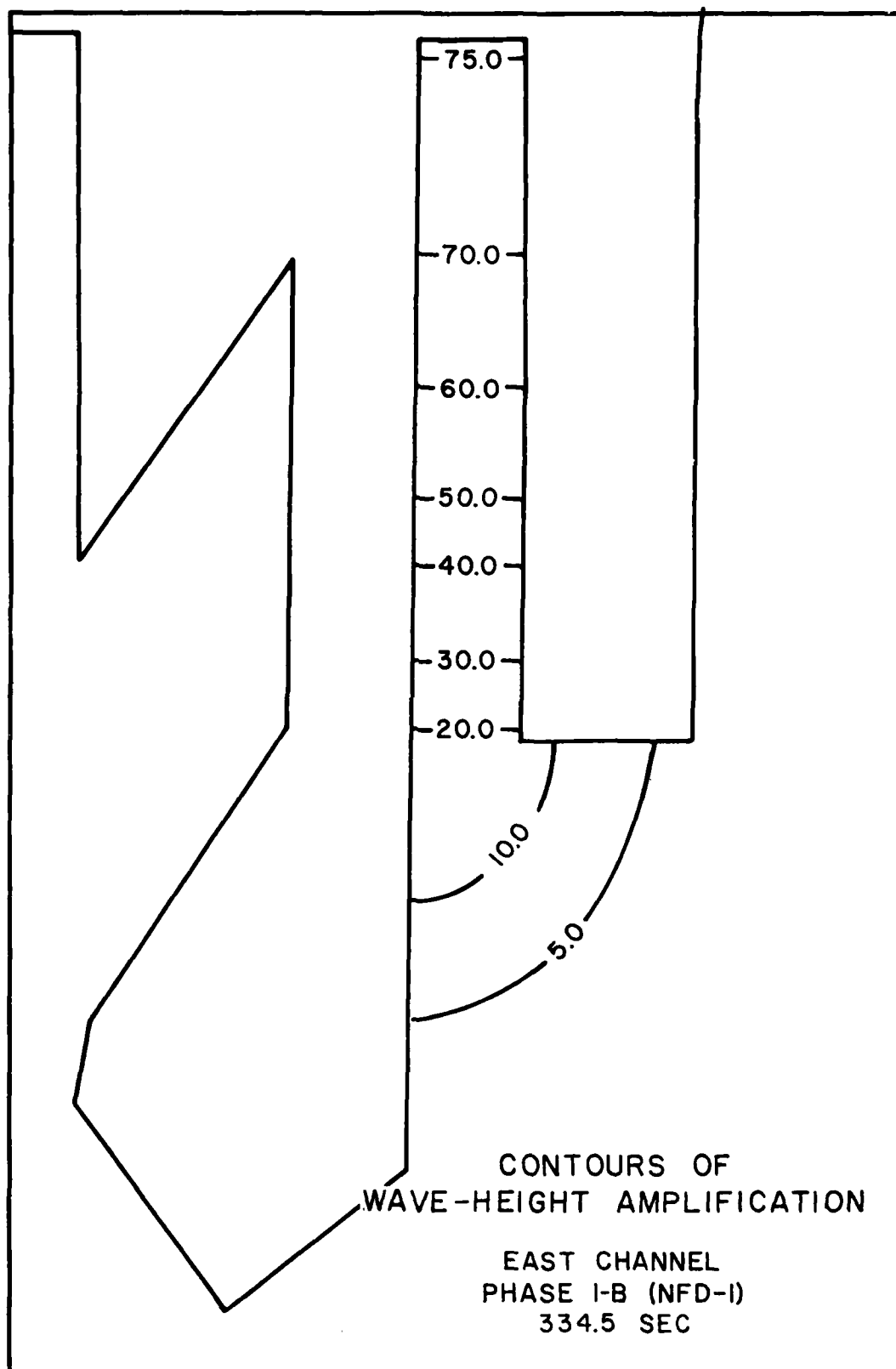
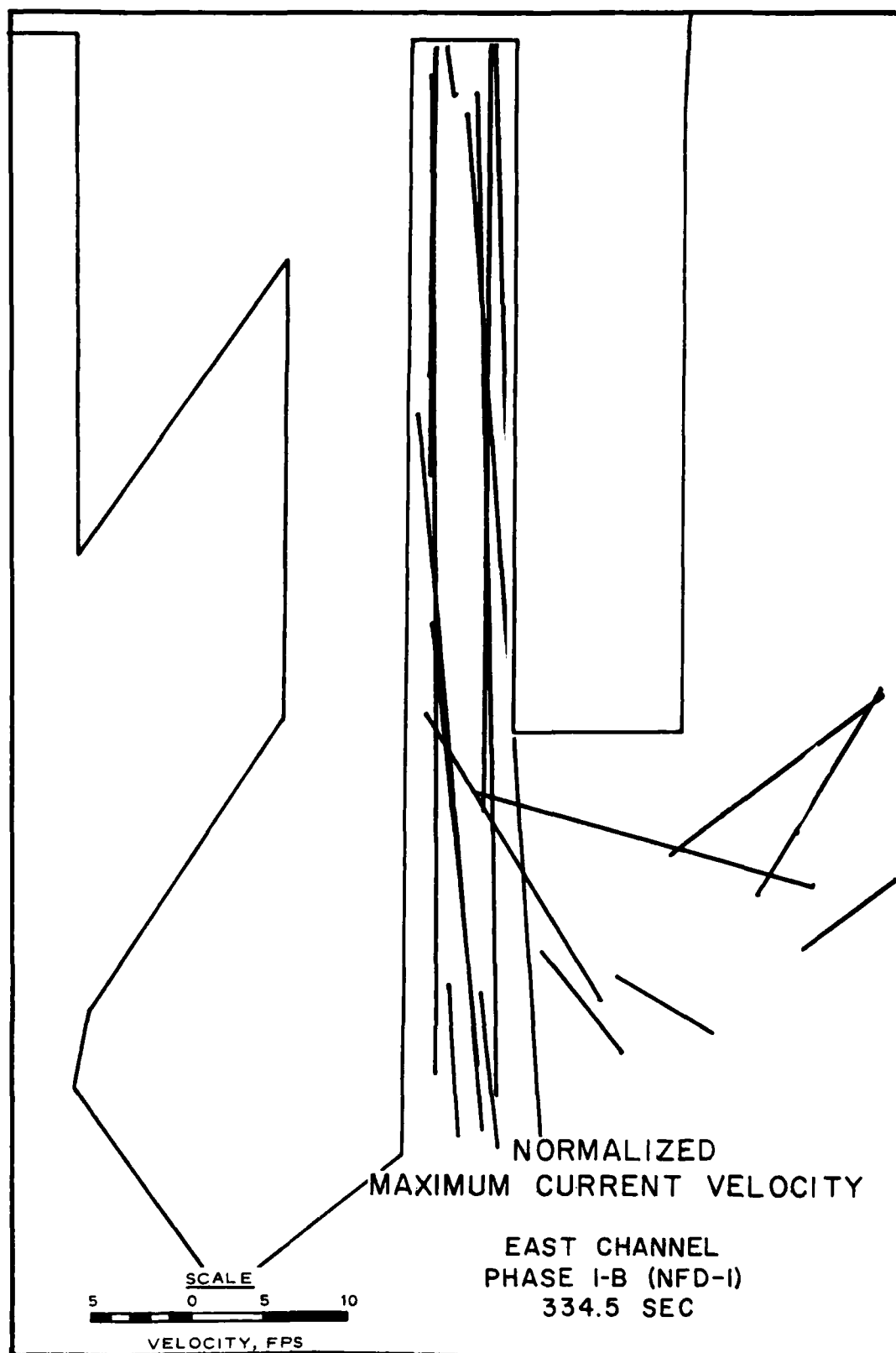
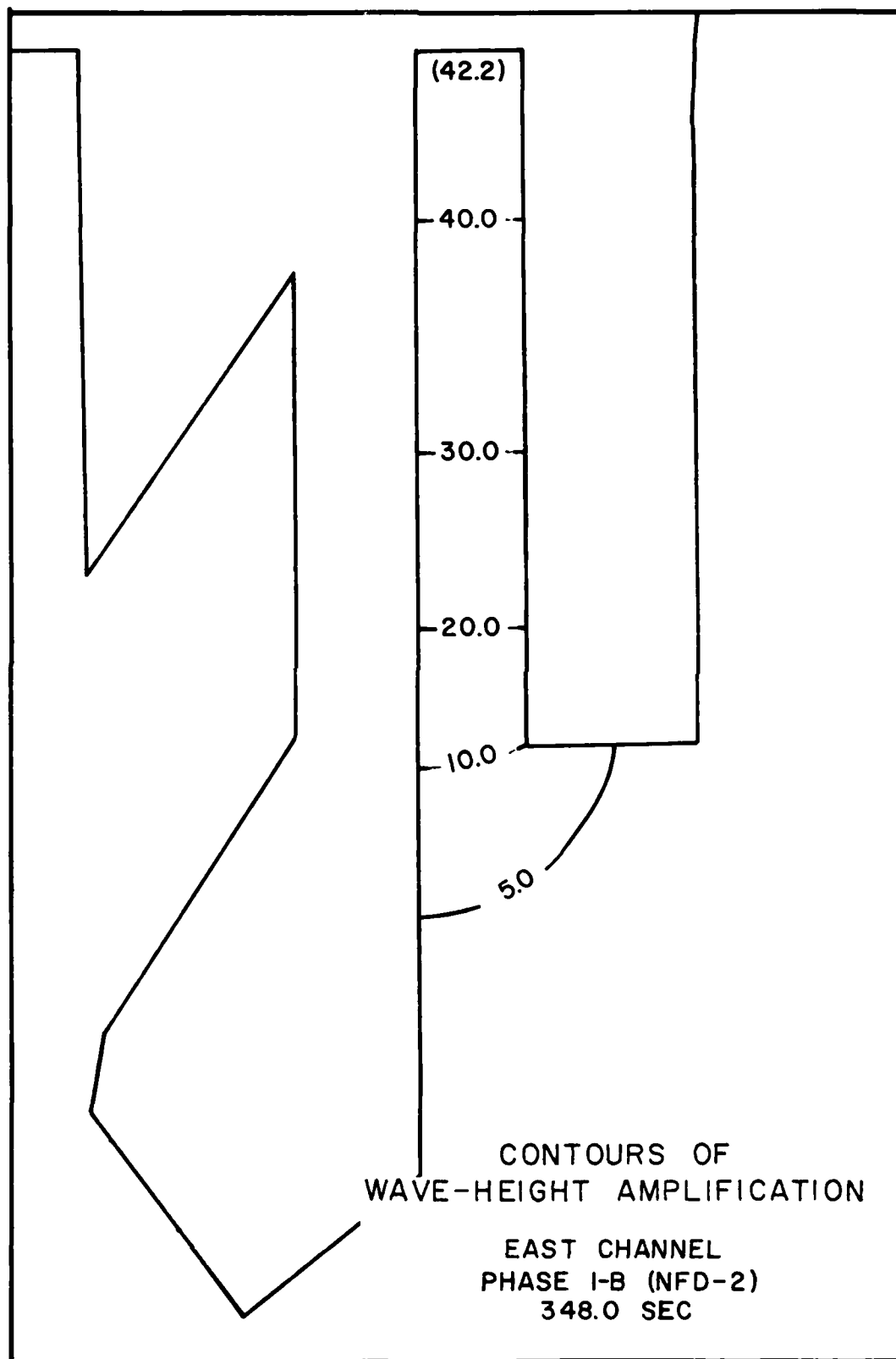
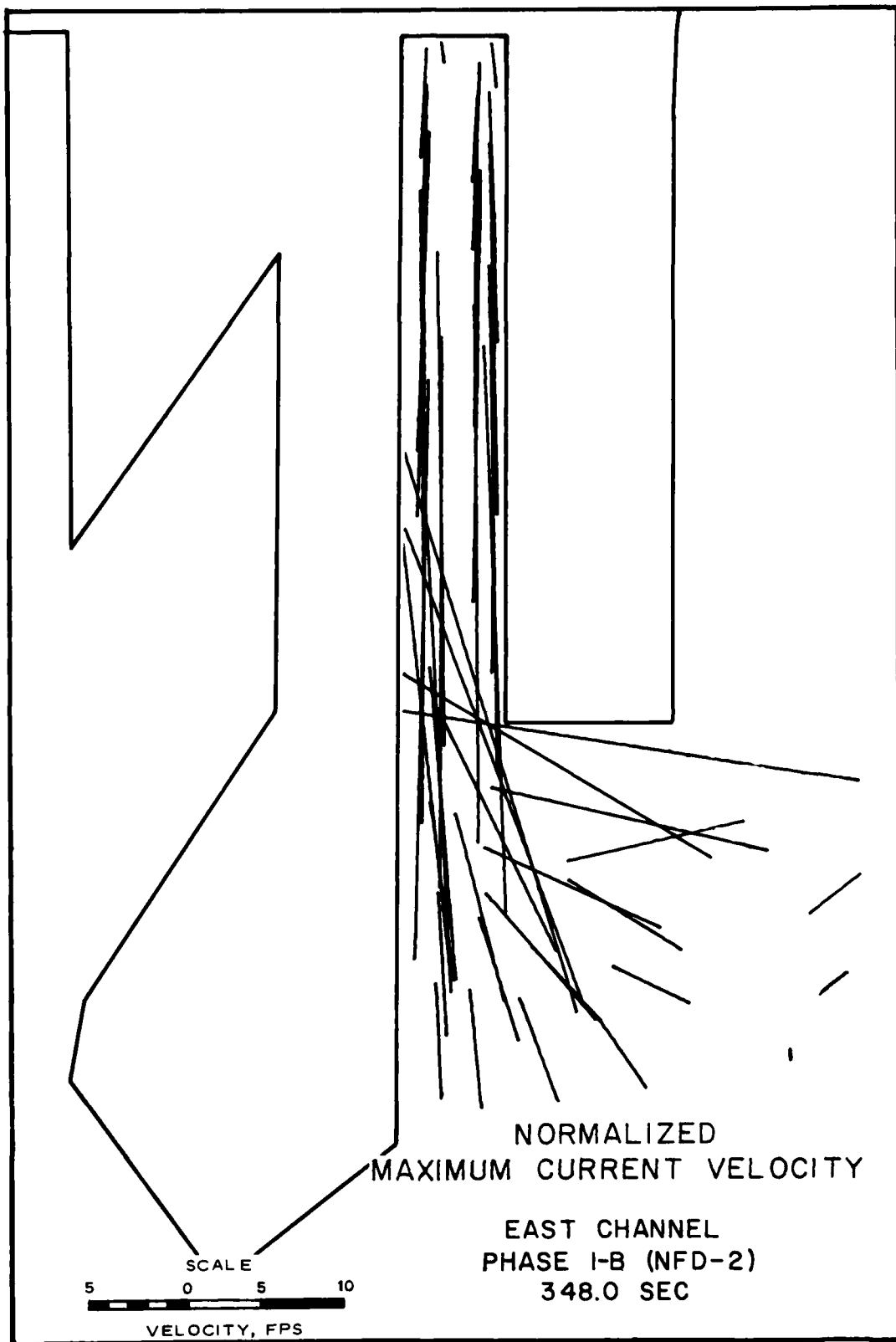


PLATE 26







APPENDIX A: NOTATION

a	Boundary of region A
A	Area of region inside a harbor
F	Functional
g	Acceleration due to gravity, 32.2 ft/sec^2
h	Water depth, ft
H_n	Hankel function of the first kind of order n
i	Imaginary number
k	Wave number, ft^{-1}
n	Integer
n_a	Unit vector normal to boundary a
r	Spherical coordinate, ft
t	Time, sec
u	Velocity in x-direction, ft/sec
U	Velocity vector
v	Velocity in y-direction, ft/sec
x	Cartesian coordinate, ft
y	Cartesian coordinate, ft
α_n	Unknown coefficient
∇	Gradient operator, ft^{-1}
η	Wave amplitude, ft
θ	Spherical coordinate, degrees
ϕ	Total velocity potential, ft^2/sec
ϕ_a	Total velocity potential evaluated on boundary a, ft^2/sec
ϕ_I	Incident velocity potential, ft^2/sec
ϕ_R	Far field velocity potential, ft^2/sec
ϕ_s	Scattered velocity potential, ft^2/sec
ω	Angular velocity, radians/sec

In accordance with letter from DAEN-RDC, DAEN-ASI dated 22 July 1977, Subject: Facsimile Catalog Cards for Laboratory Technical Publications, a facsimile catalog card in Library of Congress MARC format is reproduced below.

Outlaw, Douglas G.

Numerical analysis of harbor resonance response in East Channel, Los Angeles Harbor : final report / by Douglas G. Outlaw, James R. Houston (Hydraulics Laboratory, U.S. Army Engineer Waterways Experiment Station). -- Vicksburg, Miss. : The Station ; Springfield, Va. : available from NTIS, [1981].

16, [1] p., 29 p. of plates : ill. ; 27 cm. -- (Miscellaneous paper / U.S. Army Engineer Waterways Experiment Station ; HL-81-3)

Cover title.

"June 1981."

"Prepared for Port of Los Angeles, San Pedro, California."

1. Finite element method. 2. Los Angeles Harbor (Calif.) 3. Mathematical models. 4. Numerical analysis. I. Houston, James R. II. Port of Los Angeles. III. U.S. Army Engineer Waterways

Outlaw, Douglas G.

Numerical analysis of harbor resonance response : ... 1981.
(Card 2)

Experiment Station. Hydraulics Laboratory. IV. Title
V. Series: Miscellaneous paper (U.S. Army Engineer
Waterways Experiment Station) ; HL-81-3.
TA7.W34m no.HL-81-3